How to Survive 10 Years' Life Time for Machine Type Devices: A Study of Random Access With Sleeping-Awake Cycle

Xinghua Sun, *Member, IEEE*, Huaqiang Zhang, Wen Zhan, *Member, IEEE*, Xijun Wang, *Member, IEEE*, and Xiang Chen, *Member, IEEE*

***Abstract*— Delivering as many data packets as possible and making the life time of the network as long as possible is one fundamental request for battery-driven wireless network design, where sleeping schemes are usually adopted for prolonging the life time, while, at the sacrifice of the throughput performance. For random access networks, fulfilling this fundamental request is rather challenging due to the distributed nature of the access behavior of nodes. This paper considers massive Machine-Type Communication (mMTC) networks where each node adapts the representative random access scheme Aloha and periodical sleeping-awake cycle. We aim to address how to maximize the life-time throughput of each node, i.e., average number of packets each node can successfully deliver during its life time, with a guarantee of targeted life time via optimal selection of the channel access probability and the sleeping ratio of each node. By deriving the explicit expressions of the life time and the life-time throughput of each node and jointly tuning both the channel access probability and the sleeping ratio, we characterize the maximum life-time throughput with targeted life time, and the corresponding optimal settings. The analysis reveals that if only the channel access probability is optimally tuned, then the throughput and life-time throughput cannot be optimized simultaneously when the network becomes saturated with a large packet arrival rate. In contrast, the network would operate at unsaturated conditions via the joint tuning of the access probability and the sleeping ratio. In this case, the maximum life-time throughput always grows with the packet arrival rate. In addition, it is shown that the effect of the life-time constraint becomes significant only when it exceeds a threshold, where maximum life-time throughput will sacrifice for life-time expectation. The analysis sheds important light on the access and sleeping scheme design of practical Aloha-type networks. By taking Narrow Band-IoT with Power Saving Mode (PSM) as an example, extensive simulation results corroborate that with the proposed optimal setting, the life-time throughput could be significantly improved, especially when the life time requirement is demanding, e.g., 10 years without battery replacement.**

***Index Terms*— Aloha, life time, energy efficiency, throughput, sleeping, massive machine-type communication (mMTC).**

Manuscript received 3 January 2023; revised 9 May 2023 and 26 July 2023; accepted 28 July 2023. Date of publication 4 August 2023; date of current version 20 November 2023. This work was supported in part by National Key R&D Program of China under Grant 2022YFB2902001; in part by National Natural Science Foundation of China under Grant 62001524 and Grant 62271513; in part by the Shenzhen Science and Technology Program under Grant RCBS20210706092408010; in part by Guangdong Basic and Applied Basic Research Foundation under Grant 2021A1515012631. The associate editor coordinating the review of this article and approving it for publication was W. Liang. *(Corresponding authors: Wen Zhan; Xijun Wang.)*

Xinghua Sun, Huaqiang Zhang, and Wen Zhan are with the School of Electronics and Communication Engineering, Shenzhen Campus of Sun Yat-sen University, Shenzhen 518107, China (e-mail: sunxinghua@mail.sysu.edu.cn; zhanghq55@mail2.sysu.edu.cn; zhanw6@mail.sysu.edu.cn).

Xijun Wang and Xiang Chen are with the School of Electronics and Information Technology, Sun Yat-sen University, Guangzhou, Guangdong 510006, China (e-mail: wangxijun@mail.sysu.edu.cn; chenxiang@mail.sysu.edu.cn).

Color versions of one or more figures in this article are available at https://doi.org/10.1109/TCOMM.2023.3302133.

Digital Object Identifier 10.1109/TCOMM.2023.3302133

I. INTRODUCTION

THE ever-developing Internet of Things (IoT) promotes the ubiquitous connectivity and seamless coverage around the world, where a great number of Machine Type Devices (MTDs) work for data acquisition, processing and transmission, forming so-called Machine-to-Machine (M2M) communications [1]. The growing demands on large-scale deployments of IoT networks require each Access Point (AP) to accommodate a large number of MTDs [2]. To serve for the soaring access requests of these MTDs, the centralized access, i.e., the AP coordinates transmissions and allocates resource to each MTD, leads to intolerable overhead of scheduling, especially for small-packet and low-rate transmissions [3]. Instead, Aloha, a representative random access protocol, offers an elegant approach for MTDs to share the limited channel resources with low complexity and high scalability [4]. Aloha and its variants have been widely applied in various wireless techniques for supporting M2M communications such as Radio frequency identification (RFID), Sigfox, LoRa and so on [5].

The mMTC networks are commonly composed of small and inexpensive MTDs, which are equipped with limited battery capacity for power supply. They are usually left unattended and consequently power grid connection or recharging batteries is not feasible [6]. With stringent power constraint, yet, MTDs are expected to deliver as many packets as possible while live up to a considerable length of lifetime for the avoidance of replacement cost. One aggressive objective for ultra-low complexity MTDs is to achieve a 10 years' life time with a battery of 5 Wh [7]. Towards this end and further in consideration of sporadic data deliveries in mMTC, the sleeping mechanism provides a promising way for MTDs to save energy since the air-interfaces are switched off [8]. For instance, smart electricity meters are designed for occasional billing and system check, where MTDs are allowed to fall into

0090-6778 © 2023 IEEE. Personal use is permitted, but republication/redistribution requires IEEE permission.
See https://www.ieee.org/publications/rights/index.html for more information.

Authorized licensed use limited to: SUN YAT-SEN UNIVERSITY. Downloaded on December 14,2023 at 06:48:13 UTC from IEEE Xplore. Restrictions apply.

sleep during most of their lifetime due to low-rate sporadic traffic, e.g., less than 100 uplink events one day [9].

Moreover, the channel contention in Aloha-type mMTC network would be intensive due to the large number of MTDs, and the frequent packet collisions caused by a great amount of concurrent transmissions may result in a dramatic degradation of energy efficiency. To address this issue, besides the sleeping schedule, the backoff parameters, such as channel access probability, should also be carefully selected to avoid successive collisions, which drains battery quickly [10]. Clearly, both the sleeping schedule and the backoff parameter have significant influence on the energy efficiency and access efficiency of mMTC network. Considering the explosive growth of the number of energy-sensitive mMTC applications worldwide, it is of paramount importance to study how to properly configure the sleeping schedule and the backoff parameter in mMTC network for performance optimization and quality-of-service guarantee.

A. Related Work

1) Aloha With Sleeping Mechanisms: By putting the devices into the sleeping mode, the sleeping mechanism can prolong battery lifetime of devices and improve the energy efficiency of the network. Depending on whether the sleep/wakeup schedule is predetermined or not, we can broadly divide the sleeping protocols for Aloha networks into two categories: duty-cycled protocols and on-demand sleep/wakeup protocols.

The duty-cycled protocols require nodes to fall asleep and wake up according to a predetermined schedule, and has been used in networks, such as LoRaWAN [11]. The impact of sleep/wakeup duration on throughput and delay performance was analyzed in [12] by considering that AP was on periodic vacation. The energy efficiency of duty-cycled Aloha networks was studied with energy harvesting capability in [13], [14], [15], and [16]. In particular, it was shown in [13] that the throughput and the energy depleting probability were both strongly related to the length of active period in each duty cycle. References [14], [15], and [16] proposed energy-aware sleep/wakeup scheduling schemes to avoid energy depleting, where the packet delivery ratio, i.e., the ability of successfully delivering data from the devices to the coordinator, was analysed by allowing each node to transmit one or multiple packets per cycle. For LoRaWAN with duty-cycled Aloha, [17] developed an adaptive scheme to adjust the duty cycle in consideration of node load, network congestion rate and residual energy.

On the other hand, the on-demand sleep/wakeup protocols allows a greater flexibility as each device wakes up in an on-demand manner, e.g., upon requesting for data transmissions. It could be found in Narrow Band-IoT (NB-IoT) with Power Saving Mode (PSM)[1] [19]. The impact of PSM on energy consumption for MTDs with various packet arrival intervals were evaluated via simulations in [20]. Numerical analysis of average energy consumption in NB-IoT with PSM could be found in [21] where corresponding optimization via brute-force approach was presented. Besides, the on-demand sleep/wakeup protocols were also applied in Wake-up Radio (WuR)-based 5G networks, where the wake-up call via a dedicated channel is used to trigger data communication [22], and its energy efficiency was evaluated in [23].

Above works provided thought-provoking methods to prolong battery lifetime and achieve high energy efficiency for Aloha networks with sleeping mechanisms. Many related works, especially for the on-demand sleep/wakeup protocols, aim at proposing novel algorithms or schemes, yet, without analytical models for explicit evaluation and optimization. In particular, little attention was given on the effect of channel contention on Aloha networks with sleeping mechanisms, where backoff parameters were chosen via an empirical manner.

2) Backoff Parameter Tuning: Due to the distributed nature of the behavior of nodes in Aloha networks, transmissions from different nodes may burst out at the same time, leading to packet collisions. To control the channel contention, backoff schemes are used in Aloha right from the start. There have been a great quantity of studies on backoff parameters in Aloha networks. For instance, throughput was evaluated with geometric backoff in [24] and [25] and exponential backoff in [26], [27], and [28]. Due to the complexity, above analyses mainly focused on numerical performance analysis. An analytical framework of Aloha networks with explicit expressions to characterize network performance was proposed in [29], where an optimal transmission probability was obtained to achieve the maximum throughput.

When employed in cellular network, e.g., LTE Random Access Channel (RACH), two backoff parameters were adopted as Access Class Barring (ACB) [30], [31], i.e., the initial transmission probability and backoff window mechanism [32], i.e., a collided node randomly selects a value within the backoff window size to count down and then resumes transmission. To improve the network performance, various works were done by tuning ACB factor [33], [34], [35] and backoff window size [36], [37]. It was shown in [33] that the throughput could be optimized under delay constraint by jointly allocating ACB and the physical resource, i.e., the number of preambles and physical RACH subframes. By combining ACB and Timing Advance (TA) information, [34] alleviated the overload of RACH and then optimized the throughput. In a more realistic scenario without backlogged information, [35] derived an iterative algorithm to obtain a near-optimal ACB factor. An algorithm to estimate the number of access requests in RACH was proposed in [36], based on which the optimal backoff window size to maximize RACH throughput while satisfying the desired access success probability was obtained. With retransmission limit, i.e., the access request would be dropped when reaching the maximum retransmission limit, the throughput and the corresponding optimal backoff window size were derived in [37]. An analytical framework to combine both of the two backoff parameters was characterized in [38] and results indicated they were equally effective in optimizing the network throughput performance. The framework was

[1]NB-IoT with PSM can also operate as a duty-cycled protocol with PSM timers for periodic uplink reporting [18]. Specifically, by setting the two PSM timers of each MTD, i.e., $T3324$ and $T3412$, the duration of on-off cycle is determined, based on which each MTD could generate and transmit packets in its active state periodically. This case will be studied in section IV.

Authorized licensed use limited to: SUN YAT-SEN UNIVERSITY. Downloaded on December 14,2023 at 06:48:13 UTC from IEEE Xplore. Restrictions apply.

further extended to satisfy various delay requirements in a heterogeneous network in [39] and a distributive algorithm to obtain the optimal backoff parameters was proposed in [40].

Although extensive efforts have shed important light on access efficiency, few of them consider the energy budget, and the demand on energy efficiency would not be satisfied under the goal of access-efficiency optimization. By assuming infinite energy supply, it was shown in [41] that with careful selection of the ACB factor, the energy consumption of MTDs can be reduced up to 50%. Reference [42] proposed an analytical model to ensure devices run over an expected energy efficiency threshold by adjusting the ACB factor. Note that for many practical MTC applications, battery recharge is infeasible and the energy supply is limited. In such case, how to optimize the energy efficiency by jointly tuning the backoff parameter and the sleeping schedules are of practical importance towards the ambitious goal of surviving 10 years' lifetime.

B. Key Contributions

In this paper, we consider an n-node slotted Aloha network where all the nodes transmit to a common receiver. Each node has finite initial energy E and thus a finite life time T. To save energy, each node can enter a sleeping state, and the sleeping ratio of each node γ is introduced as the proportion of its life time spent on the sleeping state. For each node, it will wake up periodically, and has packet arrivals of mean rate λ per time slot. It will transmit packets to the receiver with access probability q if there are packets in its buffer when it is awake. The network scenario corresponds to a status update system where each node collects status information, and generates packets for information update to an access point.

To evaluate the energy efficiency, the life-time throughput of each node M, which is defined as average number of packets each node can successfully deliver during its life time, is explicitly derived and shown to be crucially determined by the access probability q and the sleeping ratio γ. We consider the life-time constrained throughput optimization problem, that is, by jointly tuning the access probability q and the sleeping ratio γ, each node is expected to live longer than a certain threshold T_0 while the life-time throughput M is maximized. The maximum life-time throughput $M_{\max}$ as well as the corresponding optimal access probability q_M and the sleeping ratio γ_M are obtained. For any fixed sleeping ratio γ, the analysis shows that the throughput and life-time throughput could be optimized simultaneously in unsaturated conditions, which will not hold in saturated conditions except when the power consumptions in all active states, i.e., transmission, waiting and idle, are the same. By jointly optimizing the access probability q and the sleeping ratio γ, in contrast, the network would always operate at unsaturated conditions and the life-time throughput grows with the packet arrival rate λ. In addition, the impact of the life-time constraint is analyzed, and a life-time threshold is characterized, beyond which the maximum life-time throughput should sacrifice for life-time expectation.

The practical insights of the analysis are demonstrated by taking the example of an NB-IoT system with PSM. In particular, it is demonstrated how to optimally select the ACB factor and PSM timers according to the optimal values of access probability q and sleeping ratio γ. It is found that the life-time throughput M could be greatly improved when applying the optimal parameters compared with the parameters chosen from the protocol. Moreover, an aggressive objective for 10-year battery life time of each low-cost/complexity MTD with limited battery capacity can be achieved when the ACB factor and duration of PSM timers are carefully tuned.

The remainder of this paper is organized as follows. Section II introduces the system model and presents a preliminary analysis. In Section III, closed-form expressions of the lifetime of each node and its life-time throughput are given, based on which the maximum life-time throughput under lifetime constraint is derived. The analysis is applied to NB-IoT, and the corresponding event-driven simulations are conducted in Section IV. Finally, conclusions are drawn in Section V.

II. System Model and Preliminary Analysis

Consider a homogeneous n-node slotted Aloha network where all the nodes transmit to a common receiver. For each node, it has a fixed amount of initial energy E, and its life ends when it runs out of energy. To save energy, each node has an independent sleep-awake cycle, and thus enters a sleeping state periodically when it can operate at a low power consumption. Define the sleeping ratio γ as the proportion of life span spent on the sleeping state. In the sleeping state, each node does not generate any packets. When it is awake, i.e., in the active state, it has packet arrivals with rate λ per time slot. This corresponds to a smart metering system, e.g., smart grid, where each device is required to report within a period periodically, and in active state, it keeps generating packets containing up-to-date information, and transmits them [43]. Assume that each node is equipped of a buffer with infinite size to accommodate packets. Each active node employs geometric retransmissions, i.e., accesses the channel at the beginning of each slot with probability q if its queue is nonempty. We assume the destructive collision channel, where concurrent packet transmissions result in collisions and decoding failure. When collided, each node would retransmit the packet until success.

An n-node buffered Aloha network can be regarded as an n-queue-single-server system, and its performance is determined by the aggregate activities of the Head-Of-Line (HOL) packets. Let us start by reviewing the throughput performance analysis of slotted Aloha in the case of $\gamma = 0$ [29], i.e., each node always keeps awake. By establishing the state transition process of each HOL packet, the probability of successful transmission of HOL packets p in the unsaturated and saturated conditions has been characterized in [29] as

$$p = \begin{cases} \exp\{\mathbb{W}_0(-n\lambda)\} & \text{if } q \in \left[\frac{-\mathbb{W}_0(-n\lambda)}{n}, \frac{-\mathbb{W}_{-1}(-n\lambda)}{n}\right] \\ \exp\{-nq\} & \text{otherwise,} \end{cases} \tag{1}$$

where $\mathbb{W}_0(\cdot)$ and $\mathbb{W}_{-1}(\cdot)$ are two branches of the Lambert W function [44]. Moreover, it is found that in the unsaturated

Authorized licensed use limited to: SUN YAT-SEN UNIVERSITY. Downloaded on December 14,2023 at 06:48:13 UTC from IEEE Xplore. Restrictions apply.

TABLE I
TABLE OF KEY NOTATIONS

Symbol	Explanation
T	Expected life time of each node.
λ_{out}	Average number of packets each node can successfully deliver per time slot in active state.
P_T, P_W, P_I and P_S	Power consumption in the transmission, waiting, idle and sleeping states, respectively
M	Average number of packets each node can successfully deliver during its life time.
p	Probability of successful transmission of HOL packets.
q	Channel access probability.
γ	Proportion of node's life time spent on the sleeping state.
p_M	Optimal probability of successful transmission of HOL packets.
q_M	Optimal channel access probability.
γ_M	Optimal sleeping ratio.
T_0	Life-time constraint.
$M^p_{\max}$	Maximum life-time throughput by tuning p with fixed γ.
$M_{\max}$	Maximum life-time throughput by jointly tuning p and γ.

case, the throughput of each node $\lambda_{\text{out}}^{\gamma=0}$, which is defined as the average number of packets each node can successfully deliver per time slot in active state, equals its packet arrival rate λ, i.e., $\lambda_{\text{out}}^{\gamma=0} = \lambda$. On the other hand, in the saturated case, the throughput of each node is given by $\lambda_{\text{out}}^{\gamma=0} = \frac{-p\ln p}{n}$. By combining these two cases, the throughput of each node is given by [29]

$$\lambda_{\text{out}}^{\gamma=0} = \begin{cases} \lambda & \text{if } p \in [\exp(\mathbb{W}_{-1}(-n\lambda)), \exp(\mathbb{W}_0(-n\lambda))] \\ \dfrac{-p\ln p}{n} & \text{otherwise.} \end{cases} \tag{2}$$

According to (2), the throughput of each node depends on the probability of successful transmission of HOL packets p. By optimizing over p, the maximum throughput of each node $\lambda_{\max}^{\gamma=0} = \max_p \lambda_{\text{out}}^{\gamma=0}$ is given by

$$\lambda_{\max}^{\gamma=0} = \min\left\{\lambda, \frac{e^{-1}}{n}\right\}. \tag{3}$$

$\lambda_{\max}^{\gamma=0}$ is achieved when $p_\lambda^{\gamma=0}$ lies in $[\exp(\mathbb{W}_{-1}(-n\lambda)), \exp(\mathbb{W}_0(-n\lambda))]$ if $\lambda \le \frac{e^{-1}}{n}$; otherwise, $\lambda_{\max}^{\gamma=0}$ is achieved when $p = p_\lambda = e^{-1}$. We would like to mention that with (1) and the optimal probability of successful transmission of HOL packets, the corresponding optimal transmission probability can also be obtained. In particular, according to $p_\lambda^{\gamma=0}$, the corresponding transmission probability q could be selected from $\left[\frac{-\mathbb{W}_0(-n\lambda)}{n}, \frac{-\mathbb{W}_{-1}(-n\lambda)}{n}\right]$ if $\lambda \le \frac{e^{-1}}{n}$ to achieve the maximum throughput $\lambda_{\max}^{\gamma=0}$. Otherwise, the transmission probability q should be $\frac{1}{n}$.

Let us now consider the case $\gamma > 0$, i.e., nodes may fall asleep. Note that in practice, the sleeping-awake cycle of each node is usually not synchronized for the release of contention. With a large number of nodes, the average number of active nodes in each time slot can be approximated as[2] $n(1-\gamma)$, with which the aggregate packet arrival rate is given by $n(1-\gamma)\lambda$. Accordingly, the throughput of each node in the active state can be given by

$$\lambda_{\text{out}} = \begin{cases} \lambda & \text{if } p \in [\exp(\mathbb{W}_{-1}(-n(1-\gamma)\lambda)), \\ & \qquad \exp(\mathbb{W}_0(-n(1-\gamma)\lambda))] \\ \dfrac{-p\ln p}{n(1-\gamma)} & \text{otherwise,} \end{cases} \tag{4}$$

[2]It can be verified according to the law of large numbers since sleeping cycle of each node is asynchronous.

and the maximum throughput of each node in the active state $\lambda_{\max} = \max\limits_p \lambda_{\text{out}}$ is given by

$$\lambda_{\max} = \min\left\{\lambda, \frac{e^{-1}}{n(1-\gamma)}\right\}. \tag{5}$$

$\lambda_{\max}$ is achieved when p_λ lies in $[\exp(\mathbb{W}_{-1}(-n(1-\gamma)\lambda)), \exp(\mathbb{W}_0(-n(1-\gamma)\lambda))]$ if $\lambda \le \frac{e^{-1}}{n(1-\gamma)}$; otherwise, $\lambda_{\max}$ is achieved when $p = p_\lambda = e^{-1}$.

Different from that in [29], this paper considers that each node has a finite amount of initial energy, and thus has a finite life span. As the homogeneous case is considered, the expected life time is identical for each node, which is denoted as T in the unit of time slots. During the life time, each node could be in the following four states: 1) transmission state, i.e., the node is transmitting packets; 2) waiting state, i.e., the node has one HOL packet waiting to access the channel; 3) idle state, i.e., the queue of the node does not have any packets; 4) sleeping state, i.e., the node is sleeping.

Let T_T, T_W, T_I and T_S denote the expected number of time slots for each node being in the transmission, waiting, idle and sleeping state during its life time, respectively. We have

$$T = T_T + T_W + T_I + T_S. \tag{6}$$

Let P_T, P_W, P_I and P_S denote the power consumption in the transmission, waiting, idle and sleeping states, respectively. For simplicity, assume that the power consumption in the idle state equals that in the waiting state, i.e., $P_I = P_W$, and thus the relation of these power consumptions is $P_S \le P_I = P_W \le P_T$. According to the total energy constraint of each node, we have

$$P_S T_S + P_W(T_I + T_W) + P_T T_T = E/\sigma, \tag{7}$$

where σ is the slot length.

Due to limited energy, each node can successfully deliver a limited number of packets during its life time, which is also a random variable. Define the life-time throughput M as the average number of packets each node can successfully deliver during its life time.[3] For quick reference, key notations in this paper are listed in Table I.

[3]Note when each packet has k information bits, the energy efficiency, which is defined as the ratio of the rate to the power consumption, can be readily obtained as $\frac{kM}{E}$, and is linear to M. Thus the life-time throughput can be regarded as a metric for energy efficiency.

Authorized licensed use limited to: SUN YAT-SEN UNIVERSITY. Downloaded on December 14,2023 at 06:48:13 UTC from IEEE Xplore. Restrictions apply.

III. Maximum Life-Time Throughput

This section aims to obtain the maximum life-time throughput of each node $M_{\max}$ and the corresponding optimal system settings. To begin with, let us derive the life-time throughput of each node M, which is the average number of packets each node can successfully deliver during its life time. Note that each node delivers packets only when it is in the active state. Define the node throughput λ_{out} as the average number of packets each node can successfully deliver when it is in the active state. Accordingly, we have

$$M = \lambda_{\text{out}}(1-\gamma)T. \tag{8}$$

The node throughput in the active state λ_{out} has been derived as a function of the probability of successful transmission of HOL packets p in (4). The following lemma presents the expression of the expected life time of each node.

Lemma 1: The expected life time of each node is given by

$$T = \begin{cases} \dfrac{E/\sigma}{\gamma P_S + (1-\gamma)\left[\frac{\lambda}{p}(P_T - P_W) + P_W\right]} \\ \qquad \text{if } p \in [\exp(\mathbb{W}_{-1}(-n(1-\gamma)\lambda)), \\ \qquad\qquad \exp(\mathbb{W}_0(-n(1-\gamma)\lambda))] \\ \dfrac{E/\sigma}{\gamma P_S + (1-\gamma)\left[\frac{-\ln p}{n(1-\gamma)}(P_T - P_W) + P_W\right]} \\ \qquad \text{otherwise.} \end{cases} \tag{9}$$

Proof: See Appendix A. ■

By combining (4), (8) and (9), the life-time throughput of each node M is given by

$$M = \begin{cases} \dfrac{E/\sigma}{\frac{P_T - P_W}{p} + \frac{P_W}{\lambda} + \frac{\gamma P_S}{\lambda(1-\gamma)}} \\ \qquad \text{if } p \in [\exp(\mathbb{W}_{-1}(-n(1-\gamma)\lambda)), \\ \qquad\qquad \exp(\mathbb{W}_0(-n(1-\gamma)\lambda))] \\ \dfrac{E/\sigma}{\frac{P_T - P_W}{p} + \frac{n(1-\gamma)(P_W + \frac{\gamma P_S}{1-\gamma})}{-p\ln p}} \qquad \text{otherwise.} \end{cases} \tag{10}$$

Let us start by analyzing a special case with $P_T = P_W$. We can see that the probability of successful transmission of HOL packets p has no effect on the lifetime T and the life-time throughput M in the unsaturated condition when letting $P_T = P_W$ in (9) and (10). The reason is that in this case, the power consumption per slot has no relation to whether the node performs data transmission or not, and only depends on whether the node falls to sleep or not.

Instead, when $P_T > P_W$, we can see from Lemma 1 that the expected life time of each node T could be improved with a larger p, which, however, may degrade the throughput performance. For instance, in an extreme case of $p = 1$, the transmission probability of each node q would approach 0 according to (4), resulting in $\lambda_{\text{out}} = 0$. As the life-time throughput of each node M is determined by both T and λ_{out}, one should strike a tradeoff between T and λ_{out} for life-time throughput maximization. Notice that such a tradeoff also exists in terms of the sleeping ratio γ. A large sleeping ratio γ prolongs the life time of each node T and relieves the channel contention. Yet the channel access opportunities is reduced as well, which deteriorates the throughput performance.

Correspondingly, we are interested in maximizing the life-time throughput of each node M by jointly tuning the probability of successful transmission of HOL packets p and the sleeping ratio γ. In practice, each node is expected to live longer than a certain threshold value in order to avoid the early death. As an example, one aggressive objective is to achieve a 10 years'life time [7]. Under such stringent constraint, we have the following constrained optimization problem[4]

$$\begin{aligned} M_{\max} = \max_{\{p,\gamma\}} \quad & M \\ s.t. \quad & T \geq T_0. \end{aligned} \tag{11}$$

The above optimization problem can be further decomposed as

$$M_{\max} = \max_{\gamma} \quad M^p_{\max}, \tag{12}$$

where

$$\begin{aligned} M^p_{\max} = \max_{p} \quad & M \\ s.t. \quad & T \geq T_0. \end{aligned} \tag{13}$$

In the following, we first look into the optimization problem (13), based on which the problem (12) is further solved.

A. Maximum Life-Time Throughput With a Given Sleeping Ratio

The following theorem presents the solution to the optimization problem (13).

Theorem 1: Given the sleeping ratio γ, the maximum life-time throughput $M^p_{\max} = \max_p M$ under the constraint of $T \geq T_0$ is given by (14), as shown at the bottom of the next page, where (15)–(16), as shown at the bottom of the next page, and

$$T_0^{*,p} = E/\sigma\Bigg(\gamma P_S + (1-\gamma) \cdot \left[\frac{\min\{\lambda, \lambda_M\}}{\exp\{\mathbb{W}_0(-n(1-\gamma)\min\{\lambda, \lambda_M\})\}}(P_T - P_W) + P_W\right]\Bigg). \tag{17}$$

Otherwise, (13) has no feasible solution. $M^p_{\max}$ is achieved when the probability of successful transmission of HOL packets p is set to be

$$p_M = \begin{cases} \exp(\mathbb{W}_0(-n(1-\gamma)\min\{\lambda, \lambda_M\})) & \text{if } T_0 \leq T_0^{*,p} \\ \exp\left\{\dfrac{-n\left[\frac{E}{\sigma T_0} + \gamma(P_W - P_S) - P_W\right]}{(P_T - P_W)}\right\} \\ \qquad \text{if } T_0^{*,p} < T_0 \leq \dfrac{E/\sigma}{P_W - (P_W - P_S)\gamma}. \end{cases} \tag{18}$$

[4]Note that with a given backoff scheme, the probability of successful transmission of HOL packets p can be obtained as a function of the channel access probability q, and thus either q or p could be chosen for the performance optimization. Here, tuning p, instead of q, gains a more general result that is independent of backoff schemes. In section IV, we will demonstrate how the optimal p can be applied to derive the optimal q with geometric retransmissions.

Authorized licensed use limited to: SUN YAT-SEN UNIVERSITY. Downloaded on December 14,2023 at 06:48:13 UTC from IEEE Xplore. Restrictions apply.

Proof: See Appendix B. ■

In particular, when $T_0 = 0$, the optimization problem (13) becomes unconstrained. In this case, the maximum life-time throughput $M_{\max}^{p,T_0=0}$ is given by

$$M_{\max}^{p,T_0=0} = \begin{cases} \dfrac{E/\sigma}{\frac{P_T - P_W}{\exp\{\mathbb{W}_0(-n(1-\gamma)\lambda)\}} + \frac{P_W}{\lambda} + \frac{\gamma P_S}{\lambda(1-\gamma)}} \\ \quad \text{if } \lambda \le \lambda_M \\ \dfrac{E/\sigma}{\frac{P_T - P_W}{\exp\{\mathbb{W}_0(-n(1-\gamma)\lambda_M)\}} + \frac{P_W}{\lambda_M} + \frac{\gamma P_S}{\lambda_M(1-\gamma)}} \\ \quad \text{otherwise,} \end{cases} \tag{19}$$

which is achieved when p is set to be

$$p_M^{T_0=0} = \begin{cases} \exp(\mathbb{W}_0(-n(1-\gamma)\lambda)) & \text{if } \lambda \le \lambda_M \\ \exp(\mathbb{W}_0(-n(1-\gamma)\lambda_M)) & \text{otherwise,} \end{cases} \tag{20}$$

according to Theorem 1.

Fig. 1a illustrates how the maximum life-time throughput $M_{\max}^{p,T_0=0}$ varies with the packet arrival rate λ with $\gamma = 0.9$ and $\frac{P_T}{P_W} = 1, 100$ or 200. It can be seen from Fig. 1a that in the unconstrained case, $M_{\max}^{p,T_0=0}$ increases as λ increases when $\lambda \le \lambda_M$. In this case, since the throughput of each node equals its packet arrival rate, $M_{\max}^{p,T_0=0}$ increases as λ increases due to a larger throughput of each node λ_{out}. As λ increases beyond λ_M, the network becomes saturated, and $M_{\max}^{p,T_0=0}$ becomes insensitive to λ. For the threshold λ_M, it increases as $\frac{P_T}{P_W}$ decreases, and reaches the largest value $\frac{e^{-1}}{n(1-\gamma)}$ when $\frac{P_T}{P_W} = 1$, as Fig. 1a illustrates.

To achieve the maximum life-time throughput $M_{\max}^{p,T_0=0}$ when $\lambda > \lambda_M$, the optimal probability of successful transmission of HOL packets $p_M^{T_0=0,\lambda>\lambda_M}$ decreases as $\frac{P_T}{P_W}$ decreases according to (20). Intuitively, with a larger $\frac{P_T}{P_W}$, each node consumes more energy for each packet transmission. In order to successfully transmit as many packets as possible with a fixed amount of initial energy, the probability of successful transmission of HOL packets should be improved. As $\frac{P_T}{P_W}$ reduces to 1, we have $p_M^{T_0=0,\lambda>\lambda_M} = e^{-1}$.

Recall that the throughput of each node λ_{out} is maximized when $p = p_\lambda = e^{-1}$ when $\lambda > \frac{e^{-1}}{n(1-\gamma)}$ according to (5), which is smaller than $p_M^{T_0=0,\lambda>\lambda_M}$ when $\frac{P_T}{P_W} > 1$, indicating a tradeoff between M and λ_{out} when $\frac{P_T}{P_W} > 1$. Notice the relation of node throughput λ_{out} and life-time throughput M is given by $M = \lambda_{\text{out}}(1-\gamma)T$ according to (8). When the throughput λ_{out} is maximized, it means that each node transmits as many as packets in each sleeping-awake cycle, which, however, may not improve the life-time throughput M as the life time of each node is reduced.

Fig. 1a further demonstrates the curve of the life-time throughput of each node M when the throughput of each node is maximized, i.e., $M|_{p=p_\lambda}$. It can be observed from Fig. 1a that if $\frac{P_T}{P_W} > 1$, then M and λ_{out} can be maximized simultaneously if and only if $\lambda \le \lambda_M$ according to (42). When $\lambda > \lambda_M$, a gap between $M_{\max}^{p,T_0=0}$ and $M|_{p=p_\lambda}$ emerges, and is enlarged as $\frac{P_T}{P_W}$ increases or λ increases, implying a more severe tradeoff between M and λ_{out}. As λ increases beyond $\frac{e^{-1}}{n(1-\gamma)}$, the maximum throughput $\lambda_{\max}$ is achieved when $p = p_\lambda = e^{-1}$ according to (5), and thus $\lambda_{\max}$ becomes a constant, i.e., $\frac{e^{-1}}{n(1-\gamma)}$, which also results in a constant of $M|_{p=p_\lambda}$ as

$$M_{\max}^{p} = \begin{cases} \dfrac{E/\sigma}{\frac{P_T - P_W}{\exp\{\mathbb{W}_0(-n(1-\gamma)\min\{\lambda,\lambda_M\})\}} + \frac{P_W}{\min\{\lambda,\lambda_M\}} + \frac{\gamma P_S}{\min\{\lambda,\lambda_M\}(1-\gamma)}} \\ \quad \text{if } \quad T_0 \le T_0^{*,p} \\ \dfrac{E/\sigma}{\frac{P_T - P_W}{\exp\{\mathbb{W}_0(-n(1-\gamma)\lambda_C)\}} + \frac{P_W + \frac{\gamma P_S}{1-\gamma}}{\lambda_C}} \\ \quad \text{if } T_0^{*,p} < T_0 \le \dfrac{E/\sigma}{P_W - (P_W - P_S)\gamma}, \end{cases} \tag{14}$$

$$\begin{aligned} \lambda_M = {} & \frac{\sqrt{(P_W + \frac{\gamma P_S}{1-\gamma})^2 + \frac{4}{n(1-\gamma)}(P_T - P_W)(P_W + \frac{\gamma P_S}{1-\gamma})} - (P_W + \frac{\gamma P_S}{1-\gamma})}{2(P_T - P_W)} \\ & \cdot \exp\left\{ \left(n(1-\gamma)(P_W + \frac{\gamma P_S}{1-\gamma}) - \left(n^2(1-\gamma)^2(P_W + \frac{\gamma P_S}{1-\gamma})^2 \right.\right.\right. \\ & \left.\left.\left. + 4n(1-\gamma)(P_T - P_W)(P_W + \frac{\gamma P_S}{1-\gamma}) \right)^{1/2} \right) / 2(P_T - P_W) \right\}, \end{aligned} \tag{15}$$

$$\begin{aligned} \lambda_C = {} & \frac{\left[\frac{E}{\sigma T_0} + \gamma(P_W - P_S) - P_W \right]}{(1-\gamma)(P_T - P_W)} \\ & \cdot \exp\left\{ \frac{-n\left[\frac{E}{\sigma T_0} + \gamma(P_W - P_S) - P_W \right]}{(P_T - P_W)} \right\}, \end{aligned} \tag{16}$$

Authorized licensed use limited to: SUN YAT-SEN UNIVERSITY. Downloaded on December 14,2023 at 06:48:13 UTC from IEEE Xplore. Restrictions apply.

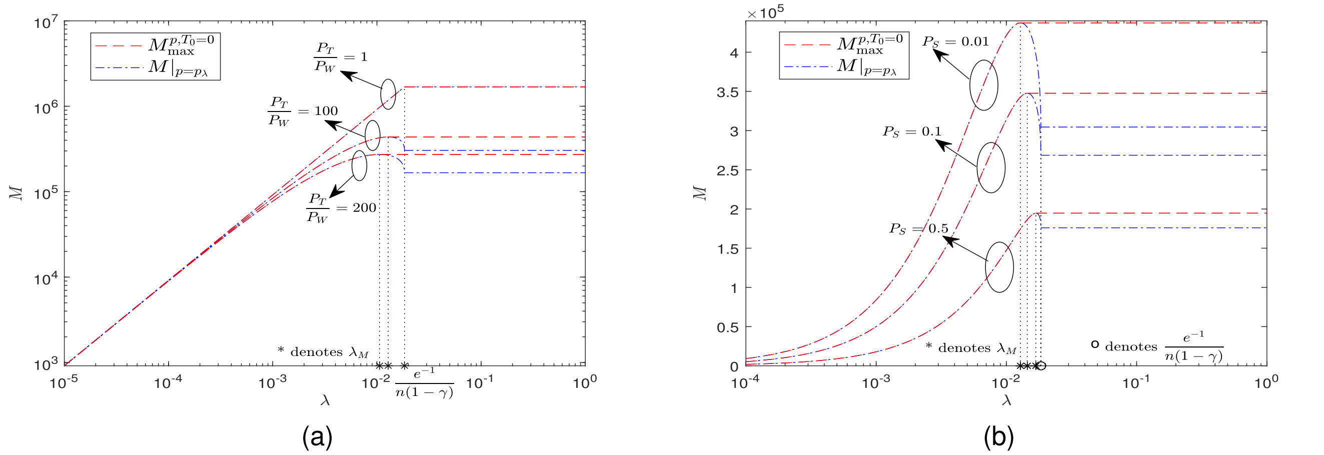

Fig. 1. The maximum life-time throughput of each node $M_{\max}^{p,T_0=0}$ versus the packet arrival rate of each node λ, $T_0 = 0$, $n = 200$, $P_W = 1$, $\gamma = 0.9$, $E/\sigma = 10^8$. (a) $P_S = 0.01$. (b) $P_T = 100$.

$M|_{p=p_\lambda} = \lambda_{\max}(1-\gamma)T$. On the other hand, if $\frac{P_T}{P_W} = 1$, then each node has the same power consumption in the transmission and waiting states. The expected life time of each node T then reduces to a constant, i.e., $T = \frac{E/\sigma}{(1-\gamma)P_W+\gamma P_S}$. Intuitively, as each node has the same power consumption when it is active, the expected life time of each node would not depend on the probability of successful transmission of HOL packets. The maximum life-time throughput $M_{\max}^{p,T_0=0}$ is then given by

$$M_{\max}^{p,T_0=0} = \frac{E/\sigma}{P_W + \frac{\gamma P_S}{1-\gamma}} \cdot \min\left\{\lambda, \frac{e^{-1}}{n(1-\gamma)}\right\}, \tag{21}$$

according to (42). In this case, M and λ_{out} can be optimized simultaneously, as Fig. 1a illustrates.

Fig. 1b illustrates how the maximum life-time throughput $M_{\max}^{p,T_0=0}$ varies with the packet arrival rate of each node λ with $P_S \in \{0.01, 0.1, 0.5\}$. It can be seen from Fig. 1b that with different values of P_S, the trend of the curves $M_{\max}^{p,T_0=0}$ versus λ is similar to that in Fig. 1a, which increases as λ increases when $\lambda \le \lambda_M$ and becomes a constant when $\lambda > \lambda_M$. For the threshold λ_M, it decreases as P_S decreases. In addition, a similar gap between $M_{\max}^{p,T_0=0}$ and $M|_{p=p_\lambda}$ occurs when $\lambda > \lambda_M$, and is enlarged as λ increases until $\lambda = \frac{e^{-1}}{n(1-\gamma)}$, indicating the tradeoff between the throughput and the life-time throughput. As $\lambda > \frac{e^{-1}}{n(1-\gamma)}$, the maximum throughput $\lambda_{\max}$ is achieved when $p = p_\lambda = e^{-1}$ according to (5), and thus $\lambda_{\max}$ becomes a constant, i.e., $\frac{e^{-1}}{n(1-\gamma)}$, which also results in a constant of $M|_{p=p_\lambda}$ as $M|_{p=p_\lambda} = \lambda_{\max}(1-\gamma)T$. Moreover, the constant gap between $M_{\max}^{p,T_0=0}$ and $M|_{p=p_\lambda}$ when $\lambda > \frac{e^{-1}}{n(1-\gamma)}$ would also be enlarged with a smaller P_S since the optimal probability of successful transmission of HOL packets probability $p_M^{T_0=0,\lambda>\lambda_M}$, which is larger than $p_\lambda = e^{-1}$, monotonically increases as P_S decreases.

Fig. 2 illustrates how the maximum life-time throughput of each node $M_{\max}^p$ varies with the life-time constraint T_0 with a fixed sleeping ratio, i.e., $\gamma = 0.9$. It can be observed from Fig. 2 that when $T_0 \le T_0^{*,p}$, $M_{\max}^p$ does not vary with T_0, which equals that without any constraint according to (42). Under such condition, since T_0 is small, the constraint $T \ge T_0$ does not have any effect on $M_{\max}^p$. As T_0 increases beyond $T_0^{*,p}$, $M_{\max}^p$ decreases as T_0 increases, and does not vary with the packet arrival rate λ as the network becomes saturated. In this case, in order to satisfy the life-time constraint T, each node would reduce the channel access probability. The corresponding optimal probability of successful transmission of HOL packets p_M, therefore, increases as T_0 increases. As T_0 approaches $\frac{E/\sigma}{(1-\gamma)P_W+\gamma P_S}$, p_M eventually approaches 1 according to (18), leading to $M_{\max}^p = 0$.

B. Maximum Life-Time Throughput With Joint Tuning

So far, with a given sleeping ratio γ, the maximum life-time throughput and the corresponding optimal probability of successful transmission of HOL packets have been characterized. In this subsection, we study how to further tune the sleeping ratio γ for maximizing the life-time throughput, i.e., addressing the optimization problem in (12).

The maximum life-time throughput $M_{\max}$ and the corresponding optimal sleeping ratio γ_M are presented in the following theorem.

Theorem 2: The maximum expected number of successfully transmitted packets in each node's life time $M_{\max}$ under the constraint of $T \ge T_0$ is given by (22), as shown at the bottom of the next page, where $\lambda_M^{\gamma=0}$ equals λ_M when $\gamma = 0$, i.e, we have

$$\lambda_M^{\gamma=0} = \frac{\sqrt{P_W^2 + \frac{4}{n}P_W(P_T - P_W)} - P_W}{2(P_T - P_W)} \cdot \exp\left\{\frac{nP_W - \sqrt{n^2P_W^2 + 4n(P_T - P_W)P_W}}{2(P_T - P_W)}\right\}, \tag{23}$$

γ_C can be derived by solving the following equation

$$\frac{(P_T - P_W)(1-\gamma_C)\mathbb{W}_0(-n(1-\gamma_C)\lambda)}{(1+\mathbb{W}_0(-n(1-\gamma_C)\lambda))\exp\{\mathbb{W}_0(-n(1-\gamma_C)\lambda)\}} = \frac{-P_s}{\lambda}, \tag{24}$$

if $\frac{(P_T-P_W)\mathbb{W}_0(-n\lambda)}{(1+\mathbb{W}_0(-n\lambda))\exp\{\mathbb{W}_0(-n\lambda)\}} + \frac{P_s}{\lambda} < 0$. Otherwise, $\gamma_C = 0$. γ_E can be obtained by solving $\lambda = \lambda_M$ according to (15), i.e., (25), as shown at the bottom of the next page.

Authorized licensed use limited to: SUN YAT-SEN UNIVERSITY. Downloaded on December 14,2023 at 06:48:13 UTC from IEEE Xplore. Restrictions apply.

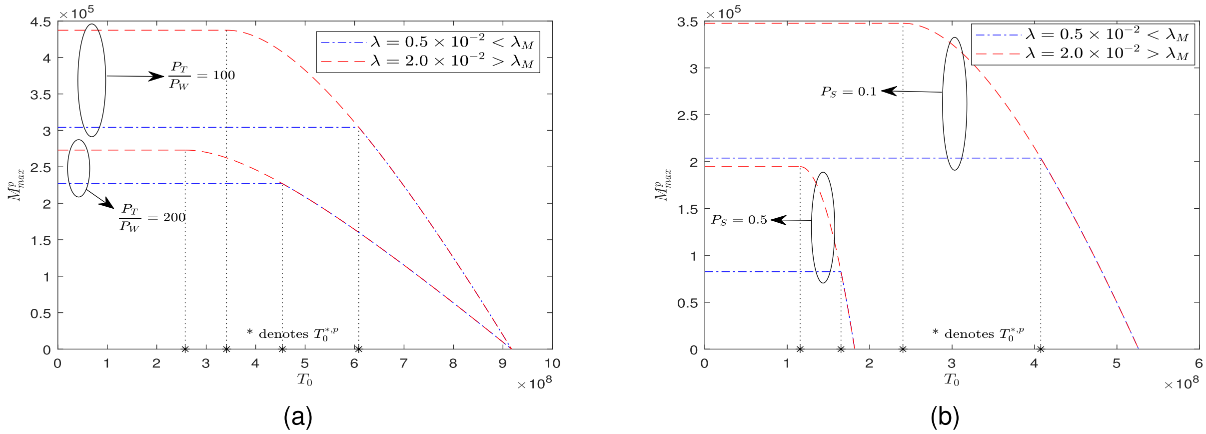

Fig. 2. The maximum life-time throughput of each node $M^p_{\max}$ versus the life-time constraint T_0. $n = 200$, $P_W = 1$, $\gamma = 0.9$, $E/\sigma = 10^8$. (a) $P_S = 0.01$. (b) $P_T = 100$.

γ_D can be obtained by solving $T_0 = T(p_M, \gamma_D)$, i.e.,

$$T_0 = \frac{E/\sigma}{\gamma_D P_S + (1-\gamma_D)\left[\frac{-\ln p_M}{n(1-\gamma_D)}(P_T - P_W) + P_W\right]}, \quad (26)$$

and T_0^* is given by (27), as shown at the bottom of the next page. Otherwise, the optimization problem (12) has no feasible solution. $M_{\max}$ is achieved when the sleeping ratio γ is set to be

$$\gamma = \gamma_M = \begin{cases} \gamma_C & \text{if } \lambda \le \lambda_M^{\gamma=0} \text{ and } T_0 \le T_0^* \\ \max\{\gamma_C, \gamma_E\} & \text{if } \lambda > \lambda_M^{\gamma=0} \text{ and } T_0 \le T_0^* \\ \gamma_D & \text{if } T_0^* < T_0 \le \dfrac{E/\sigma}{P_S}. \end{cases} \quad (28)$$

Proof: See Appendix C. ∎

Let us first consider the case of $T_0 = 0$, with which the optimization problem (12) becomes unconstrained. According to Theorem 2, the life-time throughput $M_{\max}^{T_0=0}$ is given by (29), as shown at the bottom of the next page, $M_{\max}^{T_0=0}$ is achieved when γ is set to be

$$\gamma = \gamma_M^{T_0=0} = \begin{cases} \max\{0, \gamma_C\} & \text{if } \lambda \le \lambda_M^{\gamma=0} \\ \max\{\gamma_C, \gamma_E\} & \text{otherwise.} \end{cases} \quad (30)$$

In the unconstrained case, Fig. 3 illustrates how the optimal sleeping ratio $\gamma_M^{T_0=0}$ varies with the packet arrival rate of each node λ with $\frac{P_T}{P_W} \in \{1, 100, 200\}$ and $P_S \in \{0.01, 0.1, 0.5\}$. Recall that the sleeping ratio γ denotes the proportion of life span spent on the sleeping state for each node, and also scales down the number of competing nodes in the network. When the packet arrival rate of each node λ is small, the

$$M_{\max} = \begin{cases} \dfrac{E/\sigma}{\frac{P_T - P_W}{\exp\{\mathbb{W}_0(-n(1-\gamma_C\lambda)\}} + \frac{P_W}{\lambda} + \frac{\gamma_C P_S}{\lambda(1-\gamma_C)}} \\ \qquad \text{if } \lambda \le \lambda_M^{\gamma=0} \text{ and } T_0 \le T_0^* \\ \dfrac{E/\sigma}{\frac{P_T - P_W}{\exp\{\mathbb{W}_0(-n(1-\max\{\gamma_C,\gamma_E\})\lambda)\}} + \frac{P_W}{\lambda} + \frac{\max\{\gamma_C,\gamma_E\} P_S}{\lambda(1-\max\{\gamma_C,\gamma_E\})}} \\ \qquad \text{if } \lambda > \lambda_M^{\gamma=0} \text{ and } T_0 \le T_0^* \\ \dfrac{E/\sigma}{\frac{P_T - P_W}{\exp\{\mathbb{W}_0(-n(1-\gamma_D)\lambda)\}} + \frac{P_W + \frac{\gamma_D P_S}{1-\gamma_D}}{\lambda}} \\ \qquad \text{if } T_0^* < T_0 \le \dfrac{E/\sigma}{P_S}, \end{cases} \quad (22)$$

$$\begin{aligned} \lambda = {} & \frac{\sqrt{(P_W + \frac{\gamma_E P_S}{1-\gamma_E})^2 + \frac{4}{n(1-\gamma_E)}(P_T - P_W)(P_W + \frac{\gamma_E P_S}{1-\gamma_E})} - (P_W + \frac{\gamma_E P_S}{1-\gamma_E})}{2(P_T - P_W)} \\ & \cdot \exp\Bigg\{\bigg(n(1-\gamma_E)(P_W + \frac{\gamma_E P_S}{1-\gamma_E}) - \Big(n^2(1-\gamma_E)^2 \\ & \cdot (P_W + \frac{\gamma_E P_S}{1-\gamma_E})^2 + 4n(1-\gamma_E)(P_T - P_W) \\ & \cdot (P_W + \frac{\gamma_E P_S}{1-\gamma_E})\Big)^{1/2}\bigg)/2(P_T - P_W)\Bigg\}, \end{aligned} \quad (25)$$

Authorized licensed use limited to: SUN YAT-SEN UNIVERSITY. Downloaded on December 14,2023 at 06:48:13 UTC from IEEE Xplore. Restrictions apply.

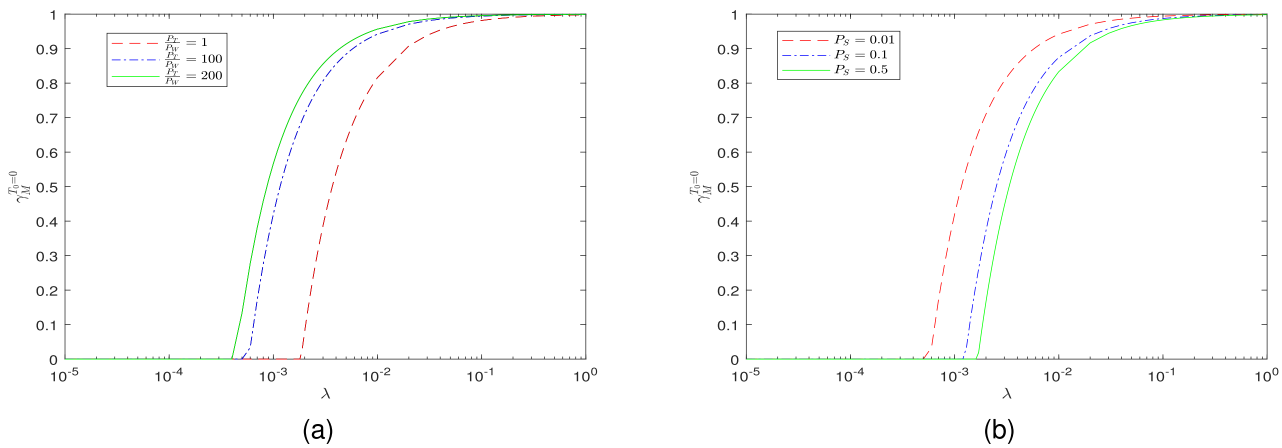

Fig. 3. The optimal sleeping ratio $\gamma_M^{T_0=0}$ versus the packet arrival rate of each node λ under the constraint $T_0 = 0$. $n = 200$, $P_W = 1$, $E/\sigma = 10^8$. (a) $P_S = 0.01$. (b) $P_T = 100$.

contention level among nodes is rather low. In this case, it can be seen from Fig. 3 that $\gamma_M^{T_0=0}$ stays at 0, indicating each node does not fall asleep at all and thus collects more packets to transmit. As λ keeps increasing, $\gamma_M^{T_0=0}$ increases, reaching its maximum when $\lambda = 1$. With a large λ, more packets will be accommodated by each node which causes more conflicts due to concurrent packet transmissions, and thus $\gamma_M^{T_0=0}$ should be enlarged to let more nodes fall into sleep at each time slot so as to alleviate the channel contention. Moreover, it can be seen from the Fig. 3a that $\gamma_M^{T_0=0}$ increases as $\frac{P_T}{P_W}$ grows since each node should sleep for more time due to larger energy consumption in the active state. For similar reason, Fig. 3b shows that when P_S increases, $\gamma_M^{T_0=0}$ should be smaller to cut down the energy consumption in the sleeping state.

Fig. 4 illustrates the corresponding maximum life-time throughput $M_{\max}^{T_0=0}$. Different from that in Fig. 1, it can be seen from Fig. 4 that $M_{\max}^{T_0=0}$ monotonically increases as λ increases. This is because when the sleeping ratio γ can be further tuned, the network can always be unsaturated by setting a large sleeping ratio. As λ increases, nevertheless, the growth of $M_{\max}^{T_0=0}$ slows down. Moreover, with a small packet arrival rate λ, each node has few packets to transmit and spends most of their life time in the idle state, and thus consumes almost the same energy regardless of different power consumptions in the transmission state. As a result, it can be observed from Fig. 4a that $M_{\max}^{T_0=0}$ does not vary with $\frac{P_T}{P_W}$ when λ is small. Similar observation can be made from Fig. 4b under different values of P_S. According to Fig. 3, with a small λ, the sleeping ratio is set to be 0 and thus the energy consumption in sleeping state P_S has no influence on the life-time throughput. As λ increases, the optimal sleeping ratio γ_M increases, leading to a greater impact of the power consumption in sleeping state P_S on the maximum life-time throughput $M_{\max}^{T_0=0}$.

Fig. 5 further illustrates how the optimal sleeping ratio γ_M varies with the life-time constraint T_0. It can be seen from Fig. 5 that when $T_0 \leq T_0^*$, γ_M does not vary with T_0, which equals the one without any constraint $\gamma_M^{T_0=0}$according to (30), indicating that with a small T_0, the life-time constraint has no impact on the life-time throughput. As T_0 increases beyond T_0^*, γ_M increases as T_0 increases, which reveals that a small

$$T_0^* = \begin{cases} \dfrac{E/\sigma}{\max\{0,\gamma_C\}P_S + (1-\max\{0,\gamma_C\})\left[\frac{-\mathbb{W}_0(-n(1-\gamma_C)\lambda)}{n(1-\max\{0,\gamma_C\})}(P_T - P_W) + P_W\right]} \\ \text{if } \lambda \leq \lambda_M^{\gamma=0} \\ \dfrac{E/\sigma}{\max\{\gamma_C,\gamma_E\}P_S + (1-\max\{\gamma_C,\gamma_E\})\left[\frac{-\mathbb{W}_0(-n(1-\gamma_C)\lambda)}{n(1-\max\{\gamma_C,\gamma_E\})}(P_T - P_W) + P_W\right]} \\ \text{otherwise.} \end{cases} \tag{27}$$

$$M_{\max}^{T_0=0} = \begin{cases} \dfrac{E/\sigma}{\frac{P_T - P_W}{\exp\{\mathbb{W}_0(-n(1-\max\{0,\gamma_C\}\lambda)\}} + \frac{P_W}{\lambda} + \frac{\max\{0,\gamma_C\}P_S}{\lambda(1-\max\{0,\gamma_C\})}} \\ \text{if } \lambda \leq \lambda_M^{\gamma=0} \\ \dfrac{E/\sigma}{\frac{P_T - P_W}{\exp\{\mathbb{W}_0(-n(1-\max\{\gamma_C,\gamma_E\})\lambda)\}} + \frac{P_W}{\lambda} + \frac{\max\{\gamma_C,\gamma_E\}P_S}{\lambda(1-\max\{\gamma_C,\gamma_E\})}} \\ \text{otherwise.} \end{cases} \tag{29}$$

Authorized licensed use limited to: SUN YAT-SEN UNIVERSITY. Downloaded on December 14,2023 at 06:48:13 UTC from IEEE Xplore. Restrictions apply.

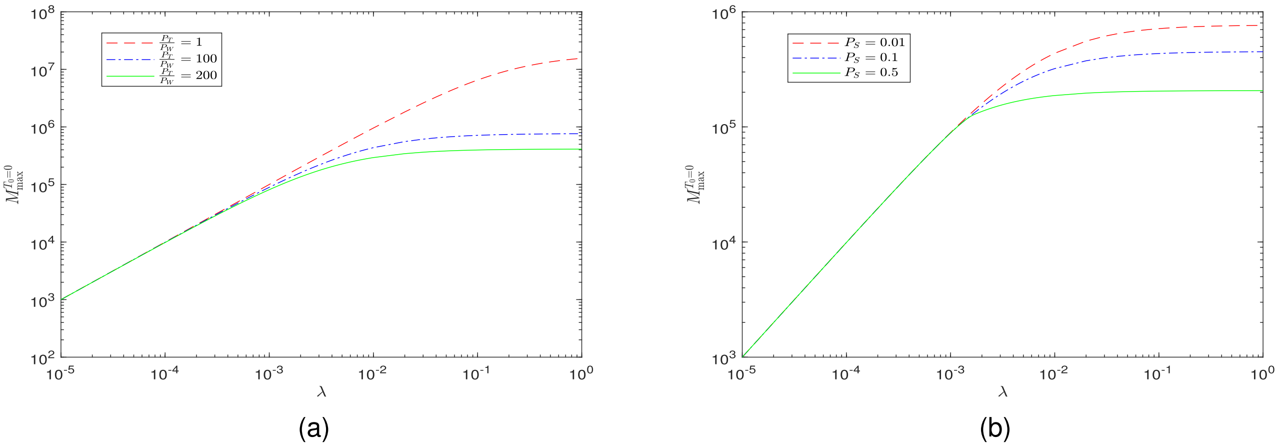

Fig. 4. The maximum life-time throughput $M_{\max}^{T_0=0}$ versus the packet arrival rate of each node λ under the constraint $T_0 = 0$. $n = 200$, $P_W = 1$, $E/\sigma = 10^8$. (a) $P_S = 0.01$. (b) $P_T = 100$.

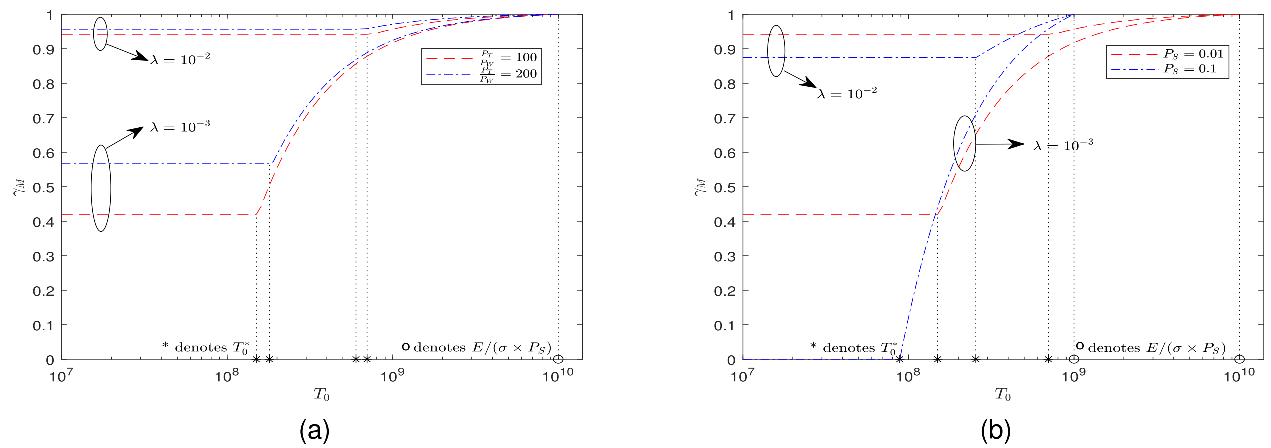

Fig. 5. The optimal sleeping ratio γ_M versus the life-time constraint T_0. $n = 200$, $P_W = 1$, $E/\sigma = 10^8$. (a) $P_S = 0.01$. (b) $P_T = 100$.

sleeping ratio is unsuitable any more since each node couldn't live up to the expected life time. Hence, due to the much lower energy consumption in the sleeping state, the sleeping ratio of each node should be enlarged enough to extend its life time.

Fig. 6 illustrates the corresponding maximum life-time throughput $M_{\max}$. According to Fig. 5, with a small T_0, i.e., $T_0 \leq T_0^*$, $M_{\max}$ equals to the one without any constraint. However, as T_0 increases beyond T_0^*, the life-time constraint will lower down the life-time throughput. In this case, $M_{\max}$ decreases as T_0 increases and finally reaches 0 when T_0 approaches $\frac{E/\sigma}{P_S}$. It can be seen from Fig. 6 that the life-time constraint $T \geq T_0$ becomes infeasible when $T_0 > \frac{E/\sigma}{P_S}$ since $\frac{E/\sigma}{P_S}$ is the longest possible life time for each node and is achieved when it is always in the sleep mode.

IV. Case Study: NB-IoT With Power Saving Mode

In this section, we will demonstrate how the proceeding analysis can be applied to practical networks by taking the example of NB-IoT with Power Saving Mode (PSM). NB-IoT was standardized by the Third-Generation Partnership Project (3GPP) to support massive machine-type communications [45], which enables a broad range of applications from mission-critical services to massive deployment of autonomous devices that periodically send state updates to remote server.

To reduce the signalling overhead, the Early Data Transmission (EDT) scheme was introduced by 3GPP, with which each Machine Type Device (MTD) can send small data packets during the random access procedure [46]. Each MTD is equipped a finite buffer size,[5] e.g., 20. Before transmitting its access request, each MTD needs to perform the Access Class Barring (ACB) check, i.e., each MTD would access the channel with transmission probability q, which is referred to as the ACB factor in standard [47]. NB-IoT with EDT can be regarded as an Aloha type network with geometric retransmission. Moreover, the power-saving mode in NB-IoT enables MTDs to set sleep and active timers. It can be seen from Fig. 7 that there are two timers used in PSM, namely T3324 and T3412 [19]. In the PSM, MTDs will enter deep sleep once the T3324 is expired and the duration of periodical on-off cycle is determined by the T3412. Therefore, the data transmission using EDT scheme in NB-IoT with PSM could be regarded as a periodical sleep-wake status update system

[5] Although an infinite buffer size is assumed, the deviation between simulation and analysis occurs only when the network is unsaturated with a quite small buffer size.

Authorized licensed use limited to: SUN YAT-SEN UNIVERSITY. Downloaded on December 14,2023 at 06:48:13 UTC from IEEE Xplore. Restrictions apply.

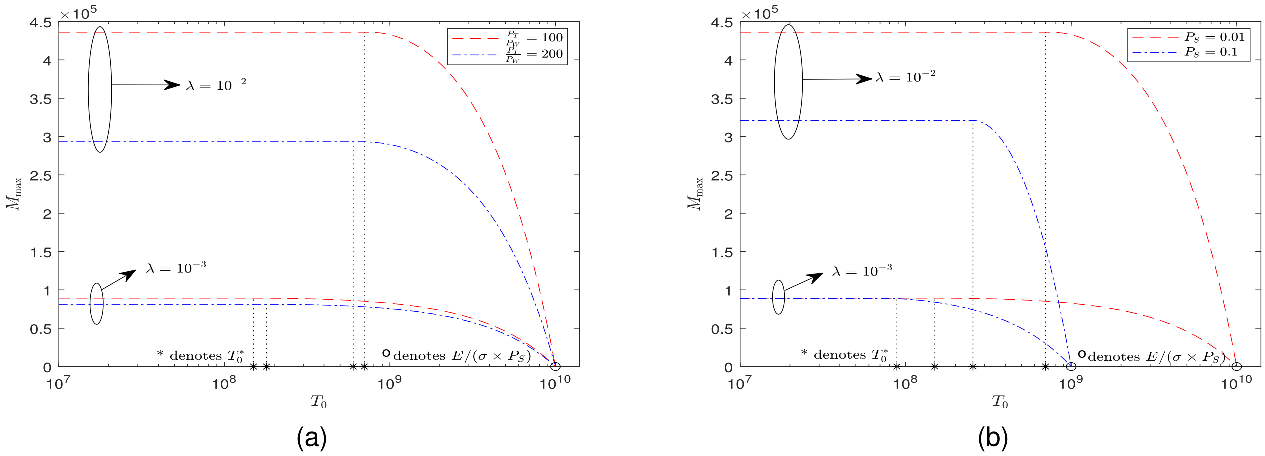

Fig. 6. The maximum life-time throughput $M_{\max}$ versus the life-time constraint T_0, $n = 200$, $P_W = 1$, $E/\sigma = 10^8$. (a) $P_S = 0.01$ (b) $P_T = 100$.

where the sleeping ratio

$$\gamma = \frac{T3412 - T3324}{T3412}. \tag{31}$$

A. Life-Time Throughput Maximization in NB-IoT

Let us consider a single-cell NB-IoT network with system parameters listed in Table II [48]. Note that in NB-IoT networks, each MTD accesses via the Physical Random Access CHannel (PRACH) to the eNB. The PRACH consists of a series of subframes that appear periodically. The time slot σ can then be defined as the interval between two consecutive PRACH subframes, which is given by $\sigma = 40$ ms according to Table II.

To be inline with the system model in Section II, we let n denote the number of MTDs. The average number of active MTDs is given by $n(1-\gamma)$. By combining (1), (9) and (10), we then have the expected life time of each MTD in unit of seconds as

$$T = \begin{cases} \dfrac{E}{\gamma P_S + (1-\gamma)\left[\frac{\lambda}{\exp\{\mathbb{W}_0(-n(1-\gamma)\lambda)\}}(P_T - P_W) + P_W\right]} \\ \quad \text{if } q \in \left[\dfrac{-\mathbb{W}_0(-n(1-\gamma)\lambda)}{n(1-\gamma)}, \dfrac{-\mathbb{W}_{-1}(-n(1-\gamma)\lambda)}{n(1-\gamma)}\right] \\ \dfrac{E}{\gamma P_S + (1-\gamma)\left[q(P_T - P_W) + P_W\right]} \\ \quad \text{otherwise,} \end{cases} \tag{32}$$

and the life-time throughput of each MTD in its life time as

$$M = \begin{cases} \dfrac{E/\sigma}{\frac{P_T - P_W}{\exp\{\mathbb{W}_0(-n(1-\gamma)\lambda)\}} + \frac{P_W}{\lambda} + \frac{\gamma P_S}{\lambda(1-\gamma)}} \\ \quad \text{if } q \in \left[\dfrac{-\mathbb{W}_0(-n(1-\gamma)\lambda)}{n(1-\gamma)}, \dfrac{-\mathbb{W}_{-1}(-n(1-\gamma)\lambda)}{n(1-\gamma)}\right] \\ \dfrac{E/\sigma}{\frac{P_T - P_W}{\exp\{-n(1-\gamma)q\}} + \frac{P_W + \frac{\gamma P_S}{1-\gamma}}{q\exp\{-n(1-\gamma)q\}}} \\ \quad \text{otherwise.} \end{cases} \tag{33}$$

TABLE II
PARAMETER SETTING [48]

Transmission power consumption P_T	545mW
Waiting and idle power consumption P_W/P_I	3mW
Sleep power consumption P_S	0.015mW
Battery capacity E	5Wh
PRACH periodicity σ	40ms

It is clear from (32) and (33) that both the expected life time T and the life-time throughput of each MTD M are determined by the ACB factor q as well as the sleeping ratio γ. In particular, with a fixed sleeping ratio γ, to achieve the maximum life-time throughput $M^p_{\max}$ under the constraint $T \geq T_0$, the optimal ACB factor is given by, (34) as shown at the bottom of the next page, according to Theorem 1. The maximum life-time throughput $M_{\max}$ with joint tuning of q and the sleeping ratio γ could be further obtained according to Theorem 2. The optimal sleeping ratio is given by (28) and the optimal ACB factor can be obtained by submitting (28) into (34).

Note that the optimal settings of ACB factor and sleeping ratio could be easily implemented in practical NB-IoT networks. Specifically, eNB can keep the record of the number of registered MTD n. The sampling rate λ and the life-time constraint T_0 depends on the applications, and could be sent to eNB through system information uploading. With n, λ and T_0, the eNB could derive the optimal settings according to (28), (31), (34) and then broadcast them to MTDs.

B. Simulation Results and Discussion

1) Life Time and Life-Time Throughput: Fig. 8 illustrates how the expected life time of each MTD T and the life-time throughput M vary with the ACB factor q with $\lambda = \{0.001, 0.01\}$ according to (32) and (33). Recall that each MTD generates packets with sampling rate λ per time slot if and only if it is awake and thus, the packets generated per on-off cycle is given by $\frac{\lambda * T3324}{\sigma}$, i.e., 2 packets per 400 seconds for $\lambda = 0.001$, $T3324 = 80\text{s}, T3412 = 400\text{s}$ and 20 packets per 400 seconds

Authorized licensed use limited to: SUN YAT-SEN UNIVERSITY. Downloaded on December 14,2023 at 06:48:13 UTC from IEEE Xplore. Restrictions apply.

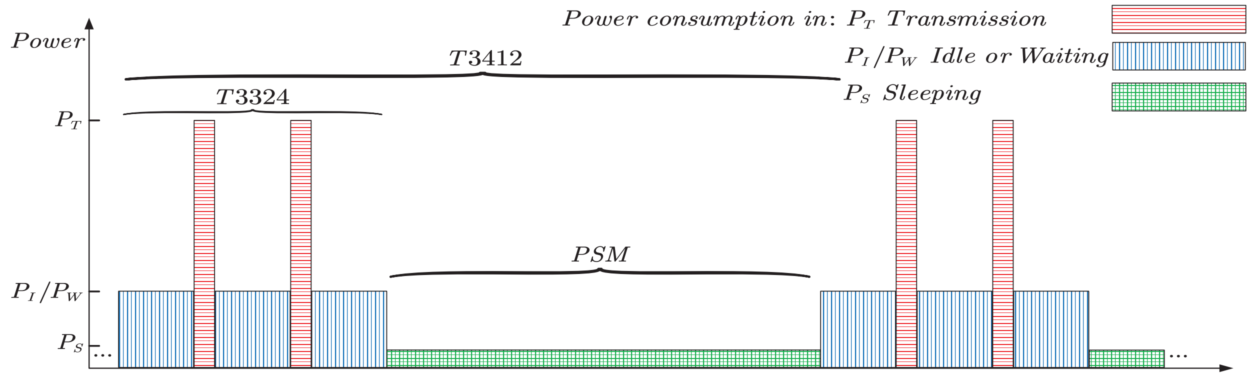

Fig. 7. Example of power consumption using EDT scheme in NB-IoT with PSM.

for $\lambda = 0.01, T3324 = 80\text{s}, T3412 = 400\text{s}$ in Fig. 8. It can be seen from the Fig. 8 that with a large sampling rate, e.g., $\lambda = 0.01$, the network is always saturated and the expected life time of each MTD T decreases as q increases, while the life-time throughput M increases as $q \le q_M = 0.0094$, decreases when $q > q_M = 0.0094$, indicating that it is maximized with $q = q_M$. On the other hand, with a small sampling rate, e.g., $\lambda = 0.001$, it could be seen from Fig. 8 that both the life time and life-time throughput remain unchanged when $q \in \left[\frac{-\mathbb{W}_0(-n(1-\gamma)\lambda)}{n(1-\gamma)}, \frac{-\mathbb{W}_{-1}(-n(1-\gamma)\lambda)}{n(1-\gamma)}\right] = [0.0010, 0.1196]$, where the network is unsaturated. Outside the region, the network becomes saturated, and the life time of each MTD T decreases as q increases, while the life-time throughput M increases as q increases when $q \le \frac{-\mathbb{W}_0(-n(1-\gamma)\lambda)}{n(1-\gamma)} = 0.0010$ and decreases as q increases when $q \ge \frac{-\mathbb{W}_{-1}(-n(1-\gamma)\lambda)}{n(1-\gamma)} = 0.1196$, indicating that the maximum M is achieved with any ACB factor q in $[0.0010, 0.1196]$.

2) Significance of Optimal Tuning: Fig. 9 demonstrates how the life-time throughput of each MTD M varies with the sampling rate of each MTD λ and $T_0 = 0$ or 2 years. Note that the ACB factor q can be chosen from the set $\{0.05, 0.1, \ldots, 0.95\}$ according to the standard [47]. Here we compare two cases: default setting of $q = 0.05$ and the optimal setting of $q = q_M$ according to (34). It can be seen from Fig. 9a that with a small λ, the life-time throughput of M with $q = q_M$ and that with $q = 0.05$ both monotonically increase as λ increases, and the gap of the two cures is negligible, since $q = 0.05$ has little deviation from the optimal set of q_M, i.e., $\left[\frac{-\mathbb{W}_0(-n(1-\gamma)\lambda)}{n(1-\gamma)}, \frac{-\mathbb{W}_{-1}(-n(1-\gamma)\lambda)}{n(1-\gamma)}\right]$ when $\lambda \le \lambda_M$ according to (34). As λ further increases beyond λ_M, the network with $q = q_M$ becomes saturated, resulting in a constant life-time throughput M. In such case, the contention in the network would be much more severe and a fixed transmission probability $q = 0.05$ would lead to the deterioration of life-time throughput. Moreover, the life-time throughput performance gap further enlarges as the PSM timer $T3324$ increases, indicating the severe collision caused by long active time. Besides the sampling rate λ, the life-time constraint T_0 also plays a key role in determining the life-time throughput performance. Note that when the life-time constraint $T > T_0$ is set, we have the sleeping ratio γ at least to be $\frac{P_W - E/T_0}{P_W - P_S}$ in order to meet the life-time constraint according to (34). With $T_0 = 2$ years in Fig. 9b, the sleeping ratio γ should be larger than 0.9094, i.e., $T3324$ less than 362.4s according to (31) with $T3412 = 400\text{s}$. Therefore, the curve of $T3324 = 800\text{s}$ and $T3324 = 400\text{s}$ disappear in Fig. 9b. It could also be seen from the dotted line in Fig. 9b that with $q = 0.05$, a more serious degradation of network performance would emerge when life-time constraint T_0 is set high in terms that MTDs cannot live up to a target lifetime when $\lambda > 0.0043$.

Recall that in Section III-B, we address how to maximize the life-time constrained throughput via jointly tuning the ACB factor q and the sleeping ratio γ. With the optimal tuning of q, Fig. 10 demonstrates how the life-time throughput of each MTD M varies with the sampling rate of each MTD λ when the sleeping ratio $\gamma = \frac{T3412 - T3324}{T3412}$ is either fixed or optimally tuned, i.e., $\frac{T3412 - T3324}{T3412} = \gamma_M$, according to (28). It can be seen from Fig. 10a that when $\frac{T3412 - T3324}{T3412} = \gamma_M$,

$$
q_M = \begin{cases} \left[\dfrac{-\mathbb{W}_0(-n(1-\gamma)\lambda)}{n(1-\gamma)}, \dfrac{-\mathbb{W}_{-1}(-n(1-\gamma)\lambda)}{n(1-\gamma)}\right] & \\ \qquad\qquad \text{if } \lambda \le \lambda_M \text{ and } T_0 \le T_0^{*,p} & \\ \dfrac{-\mathbb{W}_0(-n(1-\gamma)\lambda_M)}{n(1-\gamma)} \quad \text{if } \lambda > \lambda_M \text{ and } T_0 \le T_0^{*,p} & \\ \dfrac{\left[\frac{E}{\sigma T_0} + \gamma(P_W - P_S) - P_W\right]}{(1-\gamma)(P_T - P_W)} \text{ if } T_0^{*,p} < T_0 \le \dfrac{E}{P_W - (P_W - P_S)\gamma} & \\ \text{no solution} \qquad \text{if } T_0 > \dfrac{E}{P_W - (P_W - P_S)\gamma}, & \end{cases} \tag{34}
$$

Authorized licensed use limited to: SUN YAT-SEN UNIVERSITY. Downloaded on December 14,2023 at 06:48:13 UTC from IEEE Xplore. Restrictions apply.

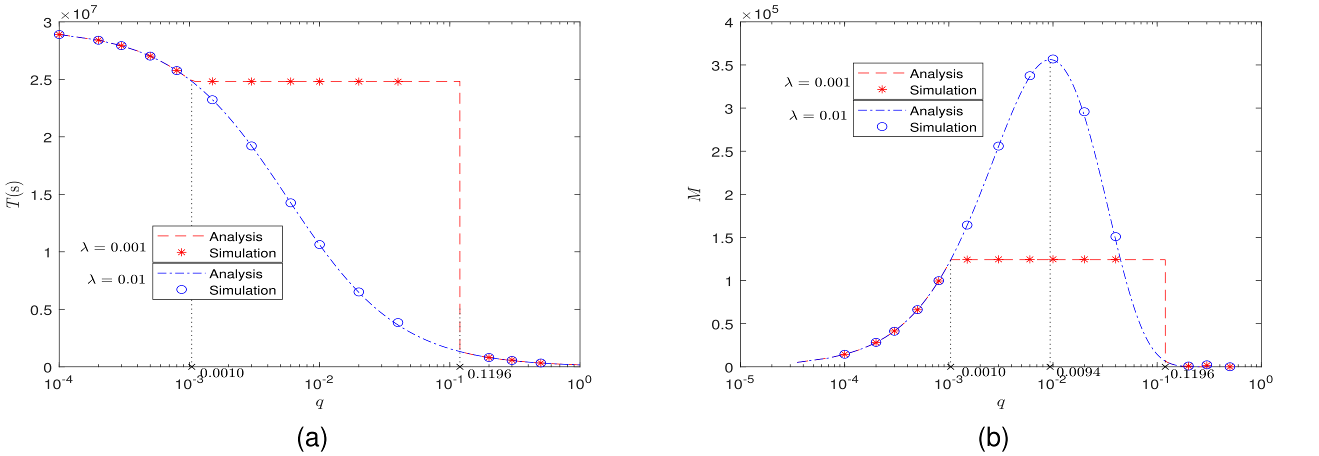

Fig. 8. (a) The expected life time of each MTD T in unit of seconds versus the ACB factor q. (b) The life-time throughput of the each MTD M versus the ACB factor q. $n = 200$, $T3412 = 400$s, $T3324 = 80$s.

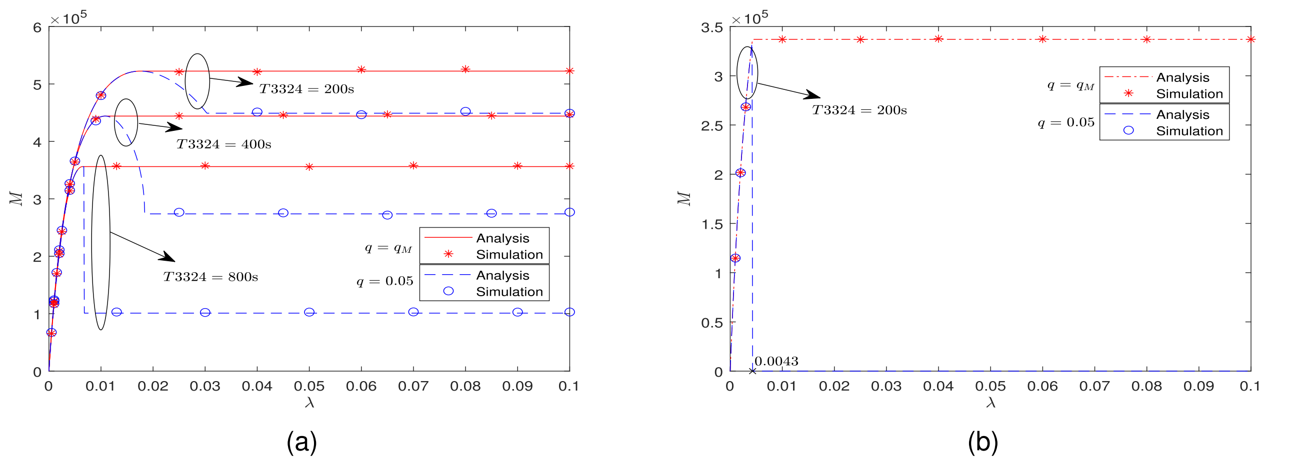

Fig. 9. The life-time throughput of each MTD M versus the sampling rate λ under the constraint $T > T_0$. $n = 200$, $T3412 = 4000$s. (a) $T_0 = 0$. (b) $T_0 = 2$ years.

the life-time throughput of each MTD M monotonically increases as the sampling rate λ increases. In this case, the network would always operate at unsaturated conditions. As Fig. 10a shows, the gap of the life-time throughput M between fixed $\frac{T3412-T3324}{T3412}$ and $\frac{T3412-T3324}{T3412} = \gamma_M$ is not visible when λ is small, while it would become obvious when the network with fixed $\frac{T3412-T3324}{T3412}$ becomes saturated with a large λ. Similar to Fig. 9b, a small sleeping ratio cannot meet the constraint $T > T_0$, resulting in the disappear of the curve of $\frac{T3412-T3324}{T3412} = 0.9$ in Fig. 10b. By comparing Fig. 10b with Fig. 10a, the gap of life-time throughput between a fixed $\frac{T3412-T3324}{T3412}$ and optimal $\frac{T3412-T3324}{T3412} = \gamma_M$ is enlarged when the life-time constraint becomes stringent, indicating great effectiveness to optimize the sleeping ratio.

3) How to Achieve 10 Years Battery Life Time?: One aggressive objective in designing NB-IoT network is to achieve a battery life time more than 10 years for each low-cost/complexity MTD equipped with a battery of 5 Wh [7]. Fig. 11 demonstrates how the maximum life-time throughput $M_{\max}$ varies with the number of MTDs n under the constraint $T_0 = 10$ years. It can be seen from Fig. 11 that the maximum life-time throughput $M_{\max}$ of each device monotonically decreases as n increases due to the collision caused by a large n, and the deterioration would become more severe with a large packet sampling rate λ. Moreover, $M_{\max}$ would increase as sampling rate λ increase since the network would always in unsaturated condition when ACB factor and the sleeping ratio are both optimized.

In the following, let us take one point in Fig. 11 as an example to illustrate how to achieve such objective based on the system parameters listed in Table II. We set $T3412 = 1$ days as the duration of the on-off cycle so that each MTD could wake up for a while per day to transmit update packets. Consider that each MTD has a sampling rate $\lambda = 0.001$, which means that it will generate one packet per 1000 time slots (40 seconds) when it is awake. With 2000 registered MTDs and life-time constraint $T_0 = 10$ years, the optimal sleeping ratio γ_M could be derived according to (28), i.e., $\gamma_M = 0.98812$ in this case. Hence, the duration of $T3324$ is given by $T3324 = T3412(1 - \gamma_M) = 1026.43$s. Moreover, by submitting γ_M into (34), the optimal ACB factor q_M could be obtained, i.e., $q_M \in [0.0010, 0.2286]$. With these optimal settings, the average life-time throughput of each MTD is up to 91747 packets, whilst the average life time could reach 10.0311 years.

Authorized licensed use limited to: SUN YAT-SEN UNIVERSITY. Downloaded on December 14,2023 at 06:48:13 UTC from IEEE Xplore. Restrictions apply.

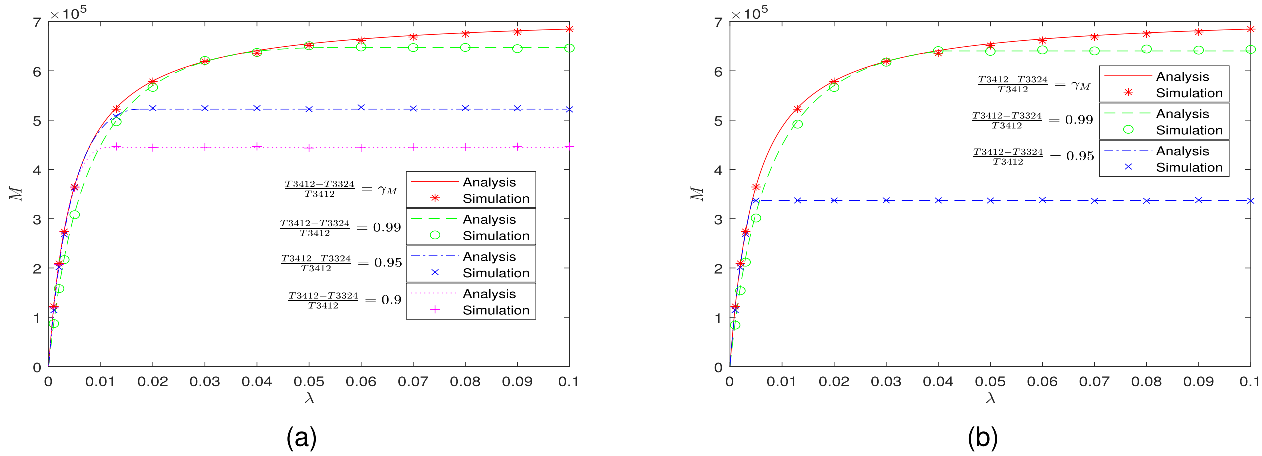

Fig. 10. The life-time throughput of each MTD M versus the sampling rate λ under the constraint $T > T_0$ when $q = q_M$. $n = 200$. (a) $T_0 = 0$. (b) $T_0 = 2$ years.

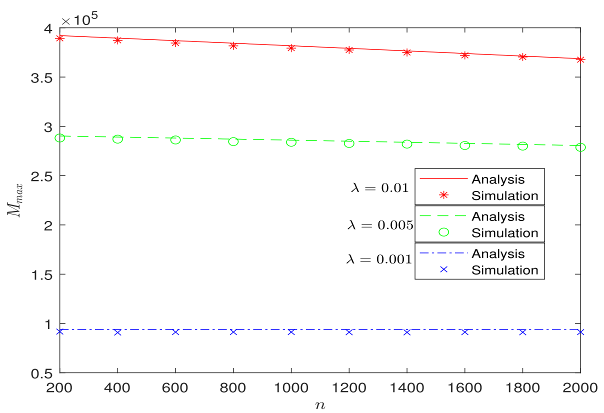

Fig. 11. Maximum life-time throughput $M_{\max}$ versus the number of MTDs n. $T_0 = 10$ years.

V. Conclusion and Future Work

This paper focuses on the energy efficiency optimization of Aloha networks with periodic sleeping-awake cycle and finite battery budget. Explicit expressions of the life time and the life-time throughput of each node are characterized, based on which the life-time constrained throughput optimization problem is addressed, i.e., maximizing the life-time throughput with life-time constraint by tuning the probability of successful transmission of HOL packets (equivalently, the channel access probability) and the sleeping ratio. The analysis reveals that with the sole tuning of the channel access probability, a severe tradeoff between the throughput and the life-time throughput performances exists, especially when the packet arrival rate is large. In contrast, these two performance metrics can be optimized simultaneously via joint tuning of the access probability and the sleeping ratio, and both are enlarged as the packet arrival rate increases. In addition, it is shown that if the life-time constraint exceeds a certain threshold, then the target life-time expectation is achieved at the expense of the deterioration of the maximum life-time throughput.

Our work provides direct guidance on performance optimization of practical Aloha networks with sleeping scheme, such as NB-IoT with PSM, where the optimal configuration of the ACB factor and the T3324/T3412 timers for life-time throughput optimization are obtained. Compared with the default system setting, significant performance improvement can be achieved via adaptive tuning. It is found that the sole tuning of the ACB factor can be applied only if the life time length requirement is not demanding. Otherwise, joint tuning of the ACB factor and the T3324/T3412 timers is necessary, particularly for achieving the 10-year life time of MTDs without battery replacement.

In this paper, we have characterized the maximum life-time throughput of each node under the constraint of its life time, while many other issues also deserve further study, such as how to maximize the life time of each node under the constraint of expected number of packets delivered in a given time span. Moreover, although the analysis in this paper has been verified via extensive simulations, developing a real-world NB-IoT network prototype and further applying our analysis in practical scenario is necessary and will also be one of our future works. Finally, this paper assumes the classical destructive collision channel. It is of great importance to extend the analysis to slotted ALOHA networks with advanced receiver structures, e.g., contention resolution diversity slotted ALOHA (CRDSA) [49] and irregular repetition slotted ALOHA (IRSA) [50].

Appendix A
Proof of Lemma 1

Based on the transmission outcome, the time in the transmission state can be further divided into the time in successful transmissions and collisions. Let T_O and T_F denote the expected numbers of time slots in successful transmissions and in collisions during each node's life time, respectively, and we have $T_T = T_O + T_F$. Note that p denotes the probability of successful transmission of HOL packets. In each channel access attempt, with probability p, one node spends one time slot in successful transmissions; otherwise, with probability $1-p$, it spends one time slot in collisions. Therefore, we have $\frac{T_O}{T_F} = \frac{p}{1-p}$. The mean service rate of each node's queue, μ, can be written as $\mu = \frac{T_O}{T_W+T_T} = \frac{p}{1+T_W/T_T}$.

$$\mu = \frac{T_O}{T_W + T_T} = \frac{p}{1 + T_W/T_T}. \tag{35}$$

Authorized licensed use limited to: SUN YAT-SEN UNIVERSITY. Downloaded on December 14,2023 at 06:48:13 UTC from IEEE Xplore. Restrictions apply.

The offered load of each node's queue, ρ, is then given by

$$\rho=\frac{\lambda}{\mu}=\frac{\lambda\left(1+T_W/T_T\right)}{p}, \tag{36}$$

where λ is the packet arrival rate of each node.

When the network is unsaturated with $\rho<1$, the offered load equals the probability that the nodes' queue is not empty. We then have

$$\frac{T_W+T_T}{T_I}=\frac{\rho}{1-\rho}. \tag{37}$$

With the sleeping ratio of each node γ, we have

$$T_S=\gamma T. \tag{38}$$

By combining (6), (7), (36), (37) and (38), we can obtain the expected life time of each node T as following

$$T=\frac{E/\sigma}{\gamma P_S+(1-\gamma)\left[\frac{\lambda}{p}(P_T-P_W)+P_W\right]}. \tag{39}$$

On the other hand, when the network becomes saturated with $\rho>1$, we have $T_I=0$. In this case, the mean service rate of each node's queue μ equals its throughput, i.e., we have

$$\mu=\lambda_{\text{out}}=\frac{-p\ln p}{n(1-\gamma)}. \tag{40}$$

By combining (6), (7), (35), (38) and (40), the expected life time of each node can be written as

$$T=\frac{E/\sigma}{\gamma P_S+(1-\gamma)\left[\frac{-\ln p}{n(1-\gamma)}(P_T-P_W)+P_W\right]}. \tag{41}$$

When $\rho=1$, it is easy to see that the expected life time of each node is also given by (41). (9) can then be obtained by combining (39) and (41).

Appendix B
Proof of Theorem 1

Lemma 2: Given the sleeping ratio γ, the maximum life-time throughput without any constraints $M_{\max}^{p,T_0=0}$ is given by

$$M_{\max}^{p,T_0=0}=\begin{cases}\dfrac{E/\sigma}{\frac{P_T-P_W}{\exp\{\mathbb{W}_0(-n(1-\gamma)\lambda)\}}+\frac{P_W}{\lambda}+\frac{\gamma P_S}{\lambda(1-\gamma)}} & \text{if } p_m\le\exp(\mathbb{W}_0(-n(1-\gamma)\lambda))\\ \dfrac{E/\sigma}{\frac{P_T-P_W}{p_m}+\frac{n(1-\gamma)(P_W+\frac{\gamma P_S}{1-\gamma})}{-p_m\ln p_m}} & \text{otherwise,}\end{cases} \tag{42}$$

where

$$p_m=\exp\left\{\left(n(1-\gamma)(P_W+\frac{\gamma P_S}{1-\gamma})-\left(n^2(1-\gamma)^2(P_W+\frac{\gamma P_S}{1-\gamma})^2+4n(1-\gamma)(P_T-P_W)(P_W+\frac{\gamma P_S}{1-\gamma})\right)^{1/2}\right)/2(P_T-P_W)\right\}. \tag{43}$$

Proof: Let $f(p)=\frac{E/\sigma}{\frac{P_T-P_W}{p}+\frac{n(1-\gamma)(P_W+\frac{\gamma P_S}{1-\gamma})}{-p\ln p}}$. If $p\notin[\exp(\mathbb{W}_{-1}(-n(1-\gamma)\lambda)),\exp(\mathbb{W}_0(-n(1-\gamma)\lambda))]$, then we have $M=f(p)$. It can be proved that $f(p)$ monotonically increases as p increases if $p<p_m$, and monotonically decreases as p increases if $p>p_m$. $f(p)$ is then maximized when $p=p_m$. It is clear that if $\lambda>\frac{e^{-1}}{n(1-\gamma)}$, then M is maximized when $p=p_m$. In the following we focus on the condition of $\lambda\le\frac{e^{-1}}{n(1-\gamma)}$. Notice that as $P_T\ge P_W$, we have $p_m\ge\exp\{-1\}\ge\exp(\mathbb{W}_{-1}(-n(1-\gamma)\lambda))$. We then divide the discussion into two cases:

1) $p_m\le\exp(\mathbb{W}_0(-n(1-\gamma)\lambda))$: This condition is equivalent to $\lambda\le\lambda_M$ according to (15). Due to the monotonicity of $f(p)$, we have $f(p)$ monotonically increases as p increases when $p<\exp(\mathbb{W}_{-1}(-n(1-\gamma)\lambda))$, and decreases as p increases when $p>\exp(\mathbb{W}_0(-n(1-\gamma)\lambda))$.
Note that $\frac{E/\sigma}{\frac{P_T-P_W}{p}+\frac{P_W}{\lambda}+\frac{\gamma P_S}{\lambda(1-\gamma)}}=f(p)$ when $p=\exp(\mathbb{W}_0(-n(1-\gamma)\lambda))$ or $p=\exp(\mathbb{W}_{-1}(-n(1-\gamma)\lambda))$, and $\frac{E/\sigma}{\frac{P_T-P_W}{p}+\frac{P_W}{\lambda}+\frac{\gamma P_S}{\lambda(1-\gamma)}}$ is a monotonically non-decreasing function of p. Therefore, M is maximized when $p=\exp(\mathbb{W}_0(-n(1-\gamma)\lambda))$.

2) $p_m>\exp(\mathbb{W}_0(-n(1-\gamma)\lambda))$: This condition is equivalent to $\lambda>\lambda_M$ according to (15). In this case, we have $M=f(p)$ if $p\notin[\exp(\mathbb{W}_{-1}(-n(1-\gamma)\lambda)),\exp(\mathbb{W}_0(-n(1-\gamma)\lambda))]$, which is maximized when $p=p_m$. If $p\in[\exp(\mathbb{W}_{-1}(-n(1-\gamma)\lambda)),\exp(\mathbb{W}_0(-n(1-\gamma)\lambda))]$, then we have $M<f(p_m)$. Therefore, M is maximized when $p=p_m$. ■

Now let us take consideration of the constraint $T\ge T_0$. According to (9), we have $T_{\max}=\max_p T=\frac{E/\sigma}{P_W-(P_W-P_S)\gamma}$. If $T_0>\frac{E/\sigma}{P_W-(P_W-P_S)\gamma}$, then the optimization problem (13) is not feasible. If $P_T=P_W$, then we have $T=\frac{E/\sigma}{P_W-(P_W-P_S)\gamma}$ according to (9). In this case, if $T_0\le\frac{E/\sigma}{P_W-(P_W-P_S)\gamma}$, then the optimization problem (13) becomes unconstrained optimization, and the solution is given by (42). When $P_T>P_W$ and $T_0\le\frac{E/\sigma}{P_W-(P_W-P_S)\gamma}$, we divide the discussion into two cases:

1) $p_m\le\exp(\mathbb{W}_0(-n(1-\gamma)\lambda))$: In this case, we have $T(\exp\{\mathbb{W}_0(-n(1-\gamma)\lambda)\})=\frac{E/\sigma}{\gamma P_S+(1-\gamma)\left[\frac{\lambda}{\exp\{\mathbb{W}_0(-n(1-\gamma)\lambda)\}}(P_T-P_W)+P_W\right]}$ according to Lemma 1, where $T(\cdot)$ is a function of p given by (9).

If $T_0\le T(\exp\{\mathbb{W}_0(-n(1-\gamma)\lambda)\})=\frac{E/\sigma}{\gamma P_S+(1-\gamma)\left[\frac{\lambda}{\exp\{\mathbb{W}_0(-n(1-\gamma)\lambda)\}}(P_T-P_W)+P_W\right]}$, then $p=\exp\{\mathbb{W}_0(-n(1-\gamma)\lambda)\}\in\{p|T\le T_0\}$, indicating that $p=\exp\{\mathbb{W}_0(-n(1-\gamma)\lambda)\}$ lies in the feasible region of the optimization problem (13). According to Case 1 of the unconstrained optimization problem, we have $M_{\max}^p=\frac{E/\sigma}{\frac{P_T-P_W}{\exp\{\mathbb{W}_0(-n(1-\gamma)\lambda)\}}+\frac{P_W}{\lambda}+\frac{\gamma P_S}{\lambda(1-\gamma)}}$, which is achieved when $p=\exp\{\mathbb{W}_0(-n(1-\gamma)\lambda)\}$.

If $T_0>T(\exp\{\mathbb{W}_0(-n(1-\gamma)\lambda)\})=\frac{E/\sigma}{\gamma P_S+(1-\gamma)\left[\frac{\lambda}{\exp\{\mathbb{W}_0(-n(1-\gamma)\lambda)\}}(P_T-P_W)+P_W\right]}$, then $T\ge T_0$ is equivalent to $p\ge p_c>\exp\{\mathbb{W}_0(-n(1-\gamma)\lambda)\}$, as T monotonically increases as p increases. As $p_m\le\exp(\mathbb{W}_0(-n(1-\gamma)\lambda))$, M monotonically decreases as

Authorized licensed use limited to: SUN YAT-SEN UNIVERSITY. Downloaded on December 14,2023 at 06:48:13 UTC from IEEE Xplore. Restrictions apply.

p increases when $p > \exp\{\mathbb{W}_0(-n(1-\gamma)\lambda)\}$. As a result, we have $M_{\max}^{p} = \frac{E/\sigma}{\frac{P_T-P_W}{\exp\{\mathbb{W}_0(-n(1-\gamma)\lambda_C)\}}+\frac{P_W+\frac{\gamma P_S}{1-\gamma}}{\lambda_C}}$, which is achieved when $p = p_c$.

2) $p_m > \exp(\mathbb{W}_0(-n(1-\gamma)\lambda))$: In this case, we have $T(p_m) = \frac{E/\sigma}{\gamma P_S+(1-\gamma)\left[\frac{\lambda_M}{\exp\{\mathbb{W}_0(-n(1-\gamma)\lambda_M)\}}(P_T-P_W)+P_W\right]}$ according to Lemma 1.

If $T_0 \leq T(p_m) = \frac{E/\sigma}{\gamma P_S+(1-\gamma)\left[\frac{\lambda_M}{\exp\{\mathbb{W}_0(-n(1-\gamma)\lambda_M)\}}(P_T-P_W)+P_W\right]}$, then $p = p_m \in \{p|T \leq T_0\}$, indicating that $p = p_m$ lies in the feasible region of the optimization problem (13). According to Case 2 of the unconstrained optimization problem, we have $M_{\max}^{p} = \frac{E/\sigma}{\frac{P_T-P_W}{\exp\{\mathbb{W}_0(-n(1-\gamma)\lambda_M)\}}+\frac{P_W}{\lambda_M}+\frac{\gamma P_S}{\lambda_M(1-\gamma)}}$, which is achieved when $p = p_m$.

If $T_0 > T(p_m) = \frac{E/\sigma}{\gamma P_S+(1-\gamma)\left[\frac{\lambda_M}{\exp\{\mathbb{W}_0(-n(1-\gamma)\lambda_M)\}}(P_T-P_W)+P_W\right]}$, then $T \geq T_0$ is equivalent to $p \geq p_c > p_m$, as T monotonically increases as p increases. As $p_m > \exp(\mathbb{W}_0(-n(1-\gamma)\lambda))$, M monotonically decreases as p increases when $p > p_m$. As a result, we have $M_{\max}^{p} = \frac{E/\sigma}{\frac{P_T-P_W}{\exp\{\mathbb{W}_0(-n(1-\gamma)\lambda_C)\}}+\frac{P_W+\frac{\gamma P_S}{1-\gamma}}{\lambda_C}}$, which is achieved when $p = p_c$.

Appendix C
Proof of Theorem 2

Theorem 1 presents the maximum life-time throughput of each node with a given fixed sleeping ratio γ. Based on Theorem 1, we further tune the sleeping ratio to optimize the life-time throughput M. Let us first derive the maximum life-time throughput $M_{\max}^{T_0=0}$ without any constraints.

Notice that $p_M^{T_0=0}$ and λ_M monotonically increase as γ increases, and thus $\lambda_M^{\max}$ and $\lambda_M^{\min}$ could be derived by converting $\gamma = 1$ and $\gamma = 0$ into (15), i.e., $\lambda_M^{\gamma=1}$ and $\lambda_M^{\gamma=0}$ respectively. Moreover, a maximum γ, i.e., $\gamma = 1$ will cause a infinite λ_M which makes the optimization problem (13) fall into situation $\lambda < \lambda_M$, definitely. According to whether λ could be larger than λ_M or not, we divide the discussion into two cases:

1) $\lambda < \lambda_M^{\gamma=0}$: In this case, we have $M_{\max p}^{T_0=0} = \frac{E/\sigma}{\frac{P_T-P_W}{\exp\{\mathbb{W}_0(-n(1-\gamma)\lambda)\}}+\frac{P_W}{\lambda}+\frac{\gamma P_S}{\lambda(1-\gamma)}}$ according to (29). Let $h(\gamma) = \frac{E/\sigma}{\frac{P_T-P_W}{\exp\{\mathbb{W}_0(-n(1-\gamma)\lambda)\}}+\frac{P_W}{\lambda}+\frac{\gamma P_S}{\lambda(1-\gamma)}}$. It can be proved that if $h'(\gamma = 0) < 0$, $h'(\gamma) = 0$ has only one zero point when $\gamma \in (0,1)$, known as $h'(\gamma_C) = 0$, where $h(\gamma)$ monotonically increases as γ increases if $\gamma < \gamma_C$, and monotonically decreases as γ increases if $\gamma > \gamma_C$. If $h'(\gamma = 0) \geq 0$, however, $h(\gamma)$ will monotonically decrease as γ increase. Therefore, $M_{\max}$ is achieved when $\gamma = \gamma_C$ or $\gamma = 0$ according to wether $h'(\gamma = 0)$ is smaller than 0 or not.

2) $\lambda \geq \lambda_M^{\gamma=0}$: In this case, we have $M_{\max p}^{T_0=0} = \frac{E/\sigma}{\frac{P_T-P_W}{\exp\{\mathbb{W}_0(-n(1-\gamma)\min\{\lambda,\lambda_M\})\}}+\frac{P_W}{\min\{\lambda,\lambda_M\}}+\frac{\gamma P_S}{\min\{\lambda,\lambda_M\}(1-\gamma)}}$ according to (29). Since λ_M monotonically increases as γ increases, λ is larger than λ_M with a small γ, leading to $M_{\max p}^{T_0=0} = \frac{E/\sigma}{\frac{P_T-P_W}{\exp\{\mathbb{W}_0(-n(1-\gamma)\lambda_M)\}}+\frac{P_W}{\lambda_M}+\frac{\gamma P_S}{\lambda_M(1-\gamma)}}$. Under such condition, $M_{\max p}^{T_0=0}$ monotonically increases as γ increases. As γ keeps increasing, λ will be smaller than λ_M, and thus we have $M_{\max p}^{T_0=0} = \frac{E/\sigma}{\frac{P_T-P_W}{\exp\{\mathbb{W}_0(-n(1-\gamma)\lambda)\}}+\frac{P_W}{\lambda}+\frac{\gamma P_S}{\lambda(1-\gamma)}}$, which is the same as Case1. According to the aforementioned analysis in Case1, we could assert that $M_{\max}$ is achieved when $\gamma = \gamma_E$ if $\gamma_E > \gamma_C$ which could be derived from $\lambda = \lambda_M$. Otherwise, $M_{\max}$ is achieved when $\gamma = \gamma_C$.

Now, let us take the constraint $T \geq T_0$ into account. After optimizing the transmission probability p in problem (13), the life time of each node T is given by $T = \frac{E/\sigma}{\gamma P_S+(1-\gamma)\left[\frac{-\ln p_M}{n(1-\gamma)}(P_T-P_W)+P_W\right]}$. Since the power consumption in sleeping state is the lowest, we have $T_{\max} = \max_{p,\gamma} T = \frac{E/\sigma}{P_S}$ by letting $\gamma = 1$. If $T_0 > \frac{E/\sigma}{P_S}$, then the optimization problem (12) is not feasible. When $T_0 \leq \frac{E/\sigma}{P_S}$, we divide the discussion into two cases:

1) $T_0 \leq T = \frac{E/\sigma}{\gamma_M^{T_0=0}P_S+(1-\gamma_M^{T_0=0})\left[\frac{-\ln p_M}{n(1-\gamma_M^{T_0=0})}(P_T-P_W)+P_W\right]}$, where $\gamma_M^{T_0=0}$ is given by (30): In this case, $\gamma = \gamma_M^{T_0=0} \in \{\gamma|T \leq T_0\}$. We then have $M_{\max} = M_{\max}^{T_0=0}$ according to the unconstraint optimization problem, which is achieved when $\gamma = \gamma_M^{T_0=0}$.

2) $T_0 > T = \frac{E/\sigma}{\gamma_M^{T_0=0}P_S+(1-\gamma_M^{T_0=0})\left[\frac{-\ln p_M}{n(1-\gamma_M^{T_0=0})}(P_T-P_W)+P_W\right]}$: Recall that in unconstraint case, if $\gamma_M^{T_0=0} = 0$, M will monotonically decreases as γ increases. Since T monotonically increases as γ increases, to meet the constraint $T \geq T_0$, we have $M_{\max} = \frac{E/\sigma}{\frac{P_T-P_W}{\exp\{\mathbb{W}_0(-n(1-\gamma_D)\lambda)\}}+\frac{P_W+\frac{\gamma_D P_S}{1-\gamma_D}}{\lambda}}$, which is achieved when $\gamma = \gamma_D$, where γ_D could be derived by solving $T_0 = \frac{E/\sigma}{\gamma_D P_S+(1-\gamma_D)\left[\frac{-\ln p_M}{n(1-\gamma_D)}(P_T-P_W)+P_W\right]}$

References

[1] P. K. Verma et al., "Machine-to-Machine (M2M) communications: A survey," *J. Netw. Comput. Appl.*, vol. 66, pp. 83–105, May 2016.

[2] N. H. Mahmood et al., "White paper on critical and massive machine type communication towards 6G," 2020, *arXiv:2004.14146*.

[3] C. Bockelmann et al., "Towards massive connectivity support for scalable mMTC communications in 5G networks," *IEEE Access*, vol. 6, pp. 28969–28992, 2018.

[4] A. Laya, L. Alonso, and J. Alonso-Zarate, "Is the random access channel of LTE and LTE-A suitable for M2M communications? A survey of alternatives," *IEEE Commun. Surveys Tuts.*, vol. 16, no. 1, pp. 4–16, 1st Quart., 2014.

[5] A. Laya, C. Kalalas, F. Vazquez-Gallego, L. Alonso, and J. Alonso-Zarate, "Goodbye, ALOHA!" *IEEE Access*, vol. 4, pp. 2029–2044, 2016.

[6] A. Aijaz and A. H. Aghvami, "Cognitive machine-to-machine communications for Internet-of-Things: A protocol stack perspective," *IEEE Internet Things J.*, vol. 2, no. 2, pp. 103–112, Apr. 2015.

[7] *Cellular System Support for Ultra-Low Complexity and Low Throughput Internet of Things (CIoT)*, document 3GPP TR 45.820, version 13.1.0, Nov. 2015.

[8] C. G. Peces, J. Eriksson, and N. Tsiftes, "Sleepy devices versus radio duty cycling: The case of lightweight M2M," *IEEE Internet Things J.*, vol. 6, no. 2, pp. 2550–2562, Apr. 2019.

[9] J. J. Nielsen, G. C. Madueño, N. K. Pratas, R. B. Sørensen, C. Stefanovic, and P. Popovski, "What can wireless cellular technologies do about the upcoming smart metering traffic?" *IEEE Commun. Mag.*, vol. 53, no. 9, pp. 41–47, Sep. 2015.

[10] E. Soltanmohammadi, K. Ghavami, and M. Naraghi-Pour, "A survey of traffic issues in machine-to-machine communications over LTE," *IEEE Internet Things J.*, vol. 3, no. 6, pp. 865–884, Dec. 2016.

Authorized licensed use limited to: SUN YAT-SEN UNIVERSITY. Downloaded on December 14,2023 at 06:48:13 UTC from IEEE Xplore. Restrictions apply.

[11] J. Haxhibeqiri, E. De Poorter, I. Moerman, and J. Hoebeke, "A survey of LoRaWAN for IoT: From technology to application," *Sensors*, vol. 18, no. 11, p. 3995, Nov. 2018.

[12] T. O. Walker, M. Tummala, and J. McEachen, "Performance analysis of slotted ALOHA with periodic server vacations for energy-efficient medium access," in *Proc. Conf. Rec. 43rd Asilomar Conf. Signals, Syst. Comput.*, Nov. 2009, pp. 429–433.

[13] F. Iannello, O. Simeone, and U. Spagnolini, "Dynamic framed-ALOHA for energy-constrained wireless sensor networks with energy harvesting," in *Proc. IEEE Global Telecommun. Conf. (GLOBECOM)*, Dec. 2010, pp. 1–6.

[14] S. Wu, Y. Chen, K. K. Chai, F. Vazquez-Gallego, and J. Alonso-Zarate, "Analysis and performance evaluation of dynamic frame slotted-ALOHA in wireless machine-to-machine networks with energy harvesting," in *Proc. IEEE Globecom Workshops (GC Wkshps)*, Dec. 2014, pp. 1081–1086.

[15] F. Vázquez-Gallego, J. Alonso-Zarate, and L. Alonso, "Reservation dynamic frame slotted-ALOHA for wireless M2M networks with energy harvesting," in *Proc. IEEE Int. Conf. Commun. (ICC)*, Jun. 2015, pp. 5985–5991.

[16] O. Briante, A. M. Mandalari, A. Molinaro, G. Ruggeri, J. Alonso-Zarate, and F. Vazquez-Gallego, "Duty-cycle optimization for machine-to-machine area networks based on frame slotted-ALOHA with energy harvesting capabilities," in *Proc. Eur. Wireless Conf.*, May 2014, pp. 1–6.

[17] T. Deng, J. Zhu, and Z. Nie, "An improved LoRaWAN protocol based on adaptive duty cycle," in *Proc. IEEE 3rd Inf. Technol. Mechatronics Eng. Conf. (ITOEC)*, Oct. 2017, pp. 1122–1125.

[18] H. Bello, X. Jian, Y. Wei, and M. Chen, "Energy-delay evaluation and optimization for NB-IoT PSM with periodic uplink reporting," *IEEE Access*, vol. 7, pp. 3074–3081, 2019.

[19] L. Feltrin et al., "Narrowband IoT: A survey on downlink and uplink perspectives," *IEEE Wireless Commun.*, vol. 26, no. 1, pp. 78–86, Feb. 2019.

[20] P. Andres-Maldonado, P. Ameigeiras, J. Prados-Garzon, J. Navarro-Ortiz, and J. M. Lopez-Soler, "Narrowband IoT data transmission procedures for massive machine-type communications," *IEEE Netw.*, vol. 31, no. 6, pp. 8–15, Nov. 2017.

[21] A. K. Sultania, C. Blondia, and J. Famaey, "Optimizing the energy-latency tradeoff in NB-IoT with PSM and eDRX," *IEEE Internet Things J.*, vol. 8, no. 15, pp. 12436–12454, Aug. 2021.

[22] D. Ghose, F. Y. Li, and V. Pla, "MAC protocols for wake-up radio: Principles, modeling and performance analysis," *IEEE Trans. Ind. Informat.*, vol. 14, no. 5, pp. 2294–2306, May 2018.

[23] N. Ullah, M. S. Chowdhury, M. Al Ameen, and K. S. Kwak, "Energy efficient MAC protocol for low-energy critical infrastructure monitoring networks using wakeup radio," *Int. J. Distrib. Sensor Netw.*, vol. 8, no. 4, Apr. 2012, Art. no. 504946.

[24] T. Wan and A. U. Sheikh, "Performance and stability analysis of buffered slotted ALOHA protocols using tagged user approach," *IEEE Trans. Veh. Technol.*, vol. 49, no. 2, pp. 582–593, Mar. 2000.

[25] J. Luo and A. Ephremides, "On the throughput, capacity, and stability regions of random multiple access," *IEEE Trans. Inf. Theory*, vol. 52, no. 6, pp. 2593–2607, Jun. 2006.

[26] D. G. Jeong and W. S. Jeon, "Performance of an exponential backoff scheme for slotted-ALOHA protocol in local wireless environment," *IEEE Trans. Veh. Technol.*, vol. 44, no. 3, pp. 470–479, Aug. 1995.

[27] B.-J. Kwak, N.-O. Song, and L. E. Miller, "Performance analysis of exponential backoff," *IEEE/ACM Trans. Netw.*, vol. 13, no. 2, pp. 343–355, Apr. 2005.

[28] L. Barletta, F. Borgonovo, and I. Filippini, "The throughput and access delay of slotted-ALOHA with exponential backoff," *IEEE/ACM Trans. Netw.*, vol. 26, no. 1, pp. 451–464, Feb. 2018.

[29] L. Dai, "Stability and delay analysis of buffered ALOHA networks," *IEEE Trans. Wireless Commun.*, vol. 11, no. 8, pp. 2707–2719, Aug. 2012.

[30] R.-G. Cheng, J. Chen, D.-W. Chen, and C.-H. Wei, "Modeling and analysis of an extended access barring algorithm for machine-type communications in LTE-A networks," *IEEE Trans. Wireless Commun.*, vol. 14, no. 6, pp. 2956–2968, Jun. 2015.

[31] I. Leyva-Mayorga, L. Tello-Oquendo, V. Pla, J. Martinez-Bauset, and V. Casares-Giner, "On the accurate performance evaluation of the LTE-A random access procedure and the access class barring scheme," *IEEE Trans. Wireless Commun.*, vol. 16, no. 12, pp. 7785–7799, Dec. 2017.

[32] J.-B. Seo and V. C. M. Leung, "Design and analysis of backoff algorithms for random access channels in UMTS-LTE and IEEE 802.16 systems," *IEEE Trans. Veh. Technol.*, vol. 60, no. 8, pp. 3975–3989, Oct. 2011.

[33] C.-Y. Oh, D. Hwang, and T.-J. Lee, "Joint access control and resource allocation for concurrent and massive access of M2M devices," *IEEE Trans. Wireless Commun.*, vol. 14, no. 8, pp. 4182–4192, Aug. 2015.

[34] Z. Wang and V. W. S. Wong, "Optimal access class barring for stationary machine type communication devices with timing advance information," *IEEE Trans. Wireless Commun.*, vol. 14, no. 10, pp. 5374–5387, Oct. 2015.

[35] S. Duan, V. Shah-Mansouri, Z. Wang, and V. W. S. Wong, "D-ACB: Adaptive congestion control algorithm for bursty M2M traffic in LTE networks," *IEEE Trans. Veh. Technol.*, vol. 65, no. 12, pp. 9847–9861, Dec. 2016.

[36] G.-Y. Lin, S.-R. Chang, and H.-Y. Wei, "Estimation and adaptation for bursty LTE random access," *IEEE Trans. Veh. Technol.*, vol. 65, no. 4, pp. 2560–2577, Apr. 2016.

[37] W. Zhan, X. Sun, X. Wang, Y. Fu, and Y. Li, "Performance optimization for massive random access of mMTC in cellular networks with preamble retransmission limit," *IEEE Trans. Veh. Technol.*, vol. 70, no. 9, pp. 8854–8867, Sep. 2021.

[38] W. Zhan and L. Dai, "Massive random access of machine-to-machine communications in LTE networks: Modeling and throughput optimization," *IEEE Trans. Wireless Commun.*, vol. 17, no. 4, pp. 2771–2785, Apr. 2018.

[39] C. Zhang, X. Sun, J. Zhang, X. Wang, S. Jin, and H. Zhu, "Throughput optimization with delay guarantee for massive random access of M2M communications in industrial IoT," *IEEE Internet Things J.*, vol. 6, no. 6, pp. 10077–10092, Dec. 2019.

[40] C. Zhang, X. Sun, J. Zhang, X. Wang, S. Jin, and H. Zhu, "Distributive throughput optimization for massive random access of M2M communications in LTE networks," *IEEE Trans. Veh. Technol.*, vol. 69, no. 10, pp. 11828–11840, Oct. 2020.

[41] Z. Zhou et al., "Energy-efficient game-theoretical random access for M2M communications in overlapped cellular networks," *Comput. Netw.*, vol. 129, pp. 493–501, Dec. 2017.

[42] H. S. Jang, H. Jin, B. C. Jung, and T. Q. S. Quek, "Versatile access control for massive IoT: Throughput, latency, and energy efficiency," *IEEE Trans. Mobile Comput.*, vol. 19, no. 8, pp. 1984–1997, Aug. 2020.

[43] J. Lloret, J. Tomas, A. Canovas, and L. Parra, "An integrated IoT architecture for smart metering," *IEEE Commun. Mag.*, vol. 54, no. 12, pp. 50–57, Dec. 2016.

[44] R. M. Corless, G. H. Gonnet, D. E. G. Hare, D. J. Jeffrey, and D. E. Knuth, "On the Lambert W function," *Adv. Comput. Math.*, vol. 5, no. 1, pp. 329–359, 1996.

[45] Y.-P. E. Wang et al., "A primer on 3GPP narrowband Internet of Things," *IEEE Commun. Mag.*, vol. 55, no. 3, pp. 117–123, Mar. 2017.

[46] A. Hoglund, D. P. Van, T. Tirronen, O. Liberg, Y. Sui, and E. A. Yavuz, "3GPP release 15 early data transmission," *IEEE Commun. Standards Mag.*, vol. 2, no. 2, pp. 90–96, Jun. 2018.

[47] *Evolved Universal Terrestrial Radio Access (E-UTRA), Radio Resource Control (RRC) Protocol Specification*, document ETSI TS 36.331, 3GPP, version 13.12.0, Release 13, Jan. 2019.

[48] *NB LTE-Battery Lifetime Evaluation*, document RP-151393, 3GPP, Sep. 2015.

[49] E. Casini, R. De Gaudenzi, and O. R. Herrero, "Contention resolution diversity slotted ALOHA (CRDSA): An enhanced random access scheme for satellite access packet networks," *IEEE Trans. Wireless Commun.*, vol. 6, no. 4, pp. 1408–1419, Apr. 2007.

[50] G. Liva, "Graph-based analysis and optimization of contention resolution diversity slotted ALOHA," *IEEE Trans. Commun.*, vol. 59, no. 2, pp. 477–487, Feb. 2011.

Authorized licensed use limited to: SUN YAT-SEN UNIVERSITY. Downloaded on December 14,2023 at 06:48:13 UTC from IEEE Xplore. Restrictions apply.

Xinghua Sun (Member, IEEE) received the B.S. degree from the Nanjing University of Posts and Telecommunications (NJUPT), China, in 2008, and the Ph.D. degree from the City University of Hong Kong (CityU), China, in 2013. In 2010, he was a Visiting Student with the National Institute for Research in Digital Science and Technology (INRIA), France. In 2013, he was a Post-Doctoral Fellow at CityU. From 2015 to 2016, he was a Post-Doctoral Fellow at the University of British Columbia, Canada. From July to August 2019, he was a Visiting Scholar at the Singapore University of Technology and Design, Singapore. From 2014 to 2018, he was an Associate Professor with NJUPT. Since 2018, he has been an Associate Professor with Sun Yat-sen University, China. He served as the technical program committee member and the organizing committee member for numerous conferences. His research interests are in the area of stochastic modeling of wireless networks and machine learning for networking.

Huaqiang Zhang received the B.E. degree in communication engineering from the School of Electronics and Communication Engineering, Sun Yat-sen University, Shenzhen Campus, Shenzhen, China, in 2023. He is currently pursuing the Ph.D. degree with the Department of Electronic Engineering, City University of Hong Kong, Hong Kong. His research interests include machine-to-machine communications, the Internet of Things, and stochastic modeling of wireless random access networks.

Wen Zhan (Member, IEEE) received the B.S. and M.S. degrees from the University of Electronic Science and Technology of China, China, in 2012 and 2015, respectively, and the Ph.D. degree from the City University of Hong Kong, China, in 2019. He was a Research Assistant and a Post-Doctoral Fellow with the City University of Hong Kong. Since 2020, he has been with the School of Electronics and Communication Engineering, Sun Yat-sen University, China, where he is currently an Assistant Professor. His research interests include the Internet of Things, modeling, and performance optimization of next-generation mobile communication systems.

Xijun Wang (Member, IEEE) received the B.S. degree (Hons.) in communications engineering from Xidian University, Xi'an, Shaanxi, China, in 2005, and the Ph.D. degree in electronic engineering from Tsinghua University, Beijing, China, in January 2012. He was an Assistant Professor from 2012 to 2015 and an Associate Professor from 2015 to 2018 with the School of Telecommunications Engineering, Xidian University. From 2015 to 2016, he was a Research Fellow with the Information Systems Technology and Design Pillar, Singapore University of Technology and Design. He is currently an Associate Professor with Sun Yat-sen University. He has published several IEEE journals and conference proceedings in the areas of wireless networks and patents related to heterogeneous networks. His current research interests include UAV communications, edge computing, and age of information. He served as the technical program committee member for numerous IEEE conferences. He was a recipient of the Best Paper Award from the IEEE ICCC 2013. He also served as the Publicity Chair for IEEE ICCC 2013 and the Technical Program Co-Chair for the Wireless Communications Systems Symposium and IEEE ICCC 2016. He is currently a reviewer for several IEEE journals. He was recognized as an Exemplary Reviewer of the IEEE Wireless Communications Letters in 2014. He is currently an Associate Editor of IEEE Access.

Xiang Chen (Member, IEEE) received the B.E. and Ph.D. degrees from the Department of Electronic Engineering, Tsinghua University, Beijing, China, in 2002 and 2008, respectively. From July 2008 to December 2014, he was with the Wireless and Mobile Communication Technology Research and Development Center (Wireless Center) and the Aerospace Center, Tsinghua University. In July 2005 and from September 2006 to April 2007, he visited NTT DoCoMo Research and Development (YRP), and Wireless Communications and Signal Processing (WCSP) Laboratory, National Tsing Hua University. Since January 2015, he has been with the School of Electronics and Information Technology, Sun Yat-sen University, where he is currently a Full Professor. His research interests mainly focus on 5G/6G wireless and mobile communication networks, and the Internet of Things (IoT).

Authorized licensed use limited to: SUN YAT-SEN UNIVERSITY. Downloaded on December 14,2023 at 06:48:13 UTC from IEEE Xplore. Restrictions apply.